Effects of Impeller-Diffuser Interaction on Centrifugal Compressor Performance

by

Neil Paul Murray

B. Eng., Mechanical & Manufacturing Engineering (2000)
Cork Institute of Technology,
Ireland

Submitted to the Department of Aeronautics and Astronautics
in partial fulfillment of the requirements for the degree of
Master of Science in Aeronautics and Astronautics

at the

Massachusetts Institute of Technology

February 2003

Signature of Author .....
Department of Aeronautics and Astronautics
January 17, 2003

Certified by .....
Choon S. Tan, PhD
Senior Research Engineer
Thesis Supervisor

Accepted by .....
Edward M. Greitzer
H.N. Slater Professor of Aeronautics and Astronautics
Chair, Committee on Graduate Students

Effects of Impeller-Diffuser Interaction on Centrifugal Compressor Performance

by

Neil Paul Murray

Submitted to the Department of Aeronautics and Astronautics
on January 21, 2003, in partial fulfillment of the requirements for the degree of
Master of Science in Aeronautics and Astronautics.

ABSTRACT

The effect of impeller-diffuser interactions in a centrifugal compressor on the performance of the stage was examined using unsteady three-dimensional Reynolds-averaged Navier-Stokes simulations. The computed results show that the interaction between the downstream diffuser pressure field and the impeller tip clearance flow can account for performance changes in the impeller. The magnitude of the performance change due to this interaction was examined for an impeller with varying tip clearance followed by a vaned or vaneless diffuser. The impact of unsteady impeller-diffuser interaction, primarily through the impeller tip clearance flow, is reflected through a time-averaged change in impeller loss, blockage and slip. The results show that there exists a tip clearance where the beneficial effect of the impeller-diffuser interaction on the impeller performance is at a maximum.

A flow feature that consists of tip flow back leakage, was shown to occur at design speed for the centrifugal compressor stage. This flow phenomenon is described as tip flow that originates in one passage, flows downstream of the impeller trailing edge and then returns to upstream of the impeller trailing edge of a neighboring passage. Such a flow feature is a source of loss in the impeller.

A hypothesis is put forth to show that changing the diffuser vane count and changing impeller-diffuser gap has an analogous effect on the impeller performance. The centrifugal compressor stage was analyzed using diffusers of different vane counts, producing an impeller performance trend similar to that when the impeller-diffuser gap was varied, thus supporting the hypothesis made. This has the implication that the effect on impeller performance associated with changing the impeller-diffuser gap and changing the diffuser vane count can be described by the non-dimensional ratio of impeller-diffuser gap to diffuser vane pitch.

A procedure is proposed and developed for isolating impeller passage blockage change without the need to define the region of blockage generation (which may incur a certain degree of arbitrariness). This method has been assessed for its applicability and utility.

Thesis Supervisor: Dr. Choon S. Tan, Senior Research Engineer
Department of Aeronautics and Astronautics

ACKNOWLEDGEMENTS

This research was funded by NASA Glenn Research Center under grant number NAG 3-2732. This funding is much appreciated.

I am indebted to a large number of people for their assistance, encouragement and support during my time at the GTL. I would in particular like to thank the following:

My thesis supervisor Dr. Choon Tan for his counsel and guidance throughout my time in the gas turbine lab. Without Choon's help and advise this thesis would not exist.

Prof. Edward Greitzer for his advice and focus especially towards the end of my research.

I would like to thank the following staff in the GTL:
Dr. Gong Yifang for his constant advice and direction. Dr. Patrick Shum for his knowledge and experience. Mr. Paul Warren for his technical support. Ms. Lori Martinez, Ms. Julie Finn, Ms. Mary McDavitt and Ms. Holly Anderson for their administrative support.

I would like to acknowledge the financial and advisory support I received from the NASA Glenn Research Center. In particular I would like to thank Dr Gary Skoch, Dr. Patricia Prahst and Dr. Louis Larosiliere.

There are a number of people outside of MIT whose assistance was invaluable both before and during my research, these are;
Prof. William Dawes (Cambridge University), Mr. Tony Fitzpatrick (C.I.T), Mr. Tony Farrell (C.I.T), Dr. Matt Cotterell (C.I.T), Mr. Peter Grehan (SIFCO), Caleb Dhanasekaran (Cambridge University).

I would like to especially thank Lin Yiben and Liu Lixian for their invaluable advice and help through all aspects of my research from coding to understanding complex concepts. 谢谢.

I would like to thank my fellow students; Sebastien Aknouche, Borislav Sirokof, Luo Jun, Andrew Luers and Trevor Ng for their technical advice. I would like to thank my office mates for making life that bit easier, Lixian, Yiben, Mathieu, Emmanuel and Isabelle and the many friends I have here in the GTL.

MIT is all work without friends and I was lucky enough to accumulate some close friends, The Brazilian, Dah-Yoh, Eamonn, Ingvar, James, Kevin and Rick.

Finally and most of all, I wish to thank Lorraine, my parents Paul and Tricia and my two brothers Stephen and Alan for their constant support.

TABLE OF CONTENTS

NOMENCLATURE

Acronyms and Abbreviations

CC	Centrifugal Compressor
CFD	Computational Fluid Dynamics
Cp	Diffuser Pressure Recovery
C_p	Specific Heat at Constant Pressure
ft	feet
GTL	Gas Turbine Laboratory
in	Inches
Kg	Kilogram
lbm	pounds
min	Minute
MIT	Massachusetts Institute of Technology
mm	Millimeter
NASA	National Aeronautics and Space Administration
PS	Pressure Side
rev	revolution
Ro	Density
rpm	revolutions per minute
sec	seconds
SECTF	Small Engine Components Test Facility
SS	Suction Side
STP	Standard Temperature and Pressure
tc	Tip Clearance

Symbols

α	Absolute flow angle from Radial
A	Area
B	Blockage
c	Chord
C	Influence Coefficient
D	Impeller Diameter
ρ	Density
f	Particular function
G	Radial Distance between Impeller Trailing Edge and Diffuser Leading Edge
L	Length Scale of the disturbance
M	Mach Number
m	Mass
m	Meter
M_r	Relative Mach number
N	Diffuser Vane Count
N	Newton
N	Rotation Speed of the Rotor, Number of Timesteps
P	Static Pressure
P_t	Total Pressure
r	Radius
R	Gas Constant
s	Entropy
S	Diffuser Vane Leading Edge Pitch
γ	Specific Heat Ratio
T	Static Temperature
t	Time
T_t	Total Temperature

U	Impeller Blade Tip Speed
V	Absolute Velocity
Vx	Velocity in x-axis, Axial Velocity in Axial Machine
Vy	Velocity in y-axis
Vz	Velocity in z-axis
W	Relative Velocity
x	Upstream Influence
δ	Displacement Thickness
θ	Slip Angle
Γ	Circulation

Subscripts

A	Area
act	Actual
av	average
B	Blocked
ψ	Availability Averaged
Δ	Difference between peak value of tip velocity with vaned diffuser and tip velocity of vaneless diffuser at trailing edge
B	Blocked
BP	Time for one Blade Passing
e	Local cutoff point
eff	Effective
r	Radial component
S	Entropy
θ	Slip Angle
t	Tangential
te	Blade Trailing Edge
TF	Through Flow Direction
TIP	At Tip of Blade

$\perp$	Orthogonal to the Through-Flow Vector
1	Impeller Leading Edge
2	Impeller Trailing Edge
3	Diffuser Leading Edge
4	Diffuser Trailing Edge

Superscripts

$'$	Disturbance

Operators

$\circ$	Flow Rate
$\overline{\quad}$	Time Averaged
$\rightarrow$	Vector Quantity

LIST OF TABLES AND FIGURES

FIGURES

TABLES

Chapter 1

Introduction and Technical Background

1.1 Motivation

Energy and economic factors motivate the need for higher efficiency turbomachinery components. The efficiency of radial turbo-machinery tends to be lower than that of axial turbo-machinery. The flow mechanisms in axial compressors have been extensively researched and the achievable performances can be considered high. Cumpsty[5] gives a range of 86-92% efficiency for axial compressors. The research on centrifugal compressors however, has not been as extensive and Johnston [15] implies that it is a lack of research and not a lack of potential that accounts for most of the efficiency shortfall in centrifugal compressors. While the efficiency of current centrifugal compressors (Cumpsty[5] gives a value of up to 86%) does not equate with axial compressors, it is important to note that the former have numerous relative advantages. These include less parts, ease of maintenance and most importantly: they can achieve higher static and total pressure rise per stage. In contrast to axial compressors, flow in centrifugal compressor passages is relatively more complex and three-dimensional.

Shum's work [21] focused on the identification of the physical parameters responsible for the observed changes in performance of a centrifugal impeller due a downstream diffuser. This thesis continues the work Shum [21] began in that it analyses and quantifies the effect of unsteadiness associated with impeller-diffuser interactions on

the performance of the impeller. Two questions of technical interest are addressed here: (1) What is the effect of changing the impeller tip clearance on centrifugal compressor performance and (2) what is the effect of downstream diffuser vane count on centrifugal compressor performance. In order to answer these questions on a quantitative basis, the following issues need to be examined:

(i) The unsteady interaction between a downstream vaned diffuser and the upstream impeller

(ii) The unsteady mechanisms that affect the performance of a centrifugal impeller

(iii) The effects of tip clearance and diffuser vane count on the time-averaged performance of the impeller.

1.2 Technical Background

1.2.1 Centrifugal Compressor

Centrifugal compressor stages consist of an impeller and diffuser. The impeller is the rotating element that applies torque to the fluid. Impellers can have a section of blade at inlet called the inducer that turns the flow at inlet from axial to radial. Highly loaded impeller stages can include splitter blades to decrease the load per blade. Splitter blades are identical to the main blades except that the leading edge is at a distance downstream of the leading edge of the impeller main blades. The reason for cutting them short is to reduce the likelihood of inlet stall due to the increase in blockage produced by blade thickness. Japikse [14] states that numerous design investigations have shown that stages with splitters can pass higher mass flows in the inducer region. Splitters are usually located at mid pitch with the leading edge downstream of the inducer. The advantage of splitters can be seen in the total amount of work that can be done on the flow in a real machine. Impeller geometries with included splitters are capable of sustaining much higher total pressure ratios.

The shroud or casing of an impeller can be fixed to the blade or can be stationary. Low-speed impellers usually have fixed shrouds while high-speed impellers have stationary shrouds that incorporate a tip clearance between the rotating blades and stationary shroud. The reason for unshrouding the impeller at high speeds is structural. The stresses produced on the blade tip of a shrouded impeller at high speeds would require the blades to be impractically thick.

The tip clearance is defined as the distance between the blade tip and shroud and it is usually given as a percentage of the local blade span. Pressure distributions on the blade forces flow from the pressure side of a blade through the tip clearance and into the suction side of the neighboring blade passage. This flow has a velocity vector that is not aligned with the main-flow vector and a tip vortex is produced which is convected downstream. The mixing of this tip vortex with the main-flow can account for a

significant amount of loss in the impeller and a subsequent reduction in the efficiency of the stage. Results from this thesis show that there is approximately a 1% drop in efficiency per % increase in tip clearance for a stage with a downstream vaneless diffuser. Figure 1-1 shows the tip vortex flow in the NASA CC3 impeller. The vortex coming from the splitter blade has a smaller core area than the main blade tip vortex due to the lower blade loading developed at the splitter (the ratio of splitter blade loading to main blade loading is approximately 0.54).

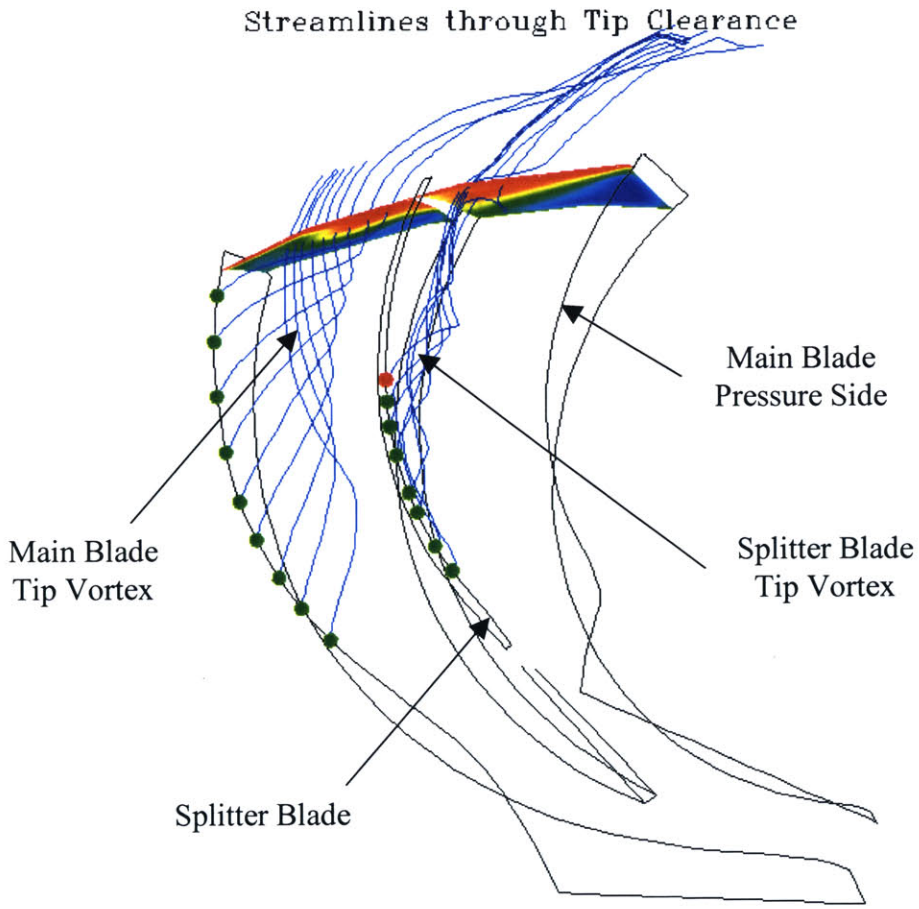

Figure 1-1 Streamlines of tip clearance flow in impeller.

The exit plane of the impeller can be designed to give purely radial flow in the rotating (relative) frame. It is often useful to 'sweep' the blades forward or backward at exit to give the relative flow a tangential component. This allows one to tailor the blade design so as to optimize the stage performance. Blades with back-sweep need a higher rotational velocity to generate a given total enthalpy rise compared to those without back-sweep because the tangential velocity at outlet is reduced. This means that with back-sweep, a higher blade tip speed is needed for a given amount of work done than for an unswept blade. This higher tip speed increases the centrifugal effect on the fluid and because the total pressure rise due to the centrifugal effect is created without losses, the efficiency of a stage with back-sweep is therefore higher than that without. Japikse[14] states that not only does a backswept impeller have a higher efficiency, it can also have an extended operating range.

The diffuser can be either vaned or vaneless. Vaned diffusers are non-rotating annular passages with a number of included blades. Vaneless diffusers as their name implies have no included blades and are thus simply annular passages. The flow through a centrifugal impeller results in a flow at the impeller exit with a high dynamic head. It is the function of the diffuser to recover the high dynamic head into static pressure. This makes the diffuser an important part of the stage. In vaneless diffusers the pressure is recovered by two mechanisms. Firstly, the area increase due to the radius change requires that the radial velocity decrease proportionally to the radius increase in order to conserve the mass flow. Secondly, the circulation (Γ) must remain constant necessitating a reduction of the tangential velocity in direct proportion to the increase in radius. In vaned diffusers, the tangential velocity is decreased rapidly by the presence of the vanes; there is also a decrease in the total velocity due to the vane passage area increase.

Unsteadiness in the rotating frame is introduced with a vaned diffuser. This is an idealized viewpoint as in reality even stages with vaneless diffusers have sources of unsteadiness such as separation. Various wake shedding effects can be seen in real machines and computationally these can be captured using high-resolution Computational Fluid Dynamics (CFD) routines. Here, vaneless diffuser stages will be deemed 'steady'.

1.2.2 Compressor Description

In this thesis, the CC3 impeller-diffuser stage will be used as a research article for addressing the two questions posed in section 1.1. This centrifugal compressor is the test stage in the test cell located in the Small Engine Components Test Facility (SECTF) at NASA Glenn Research Center, Cleveland, Ohio (see figure 1-2). The compressor has a 4:1 pressure ratio at a 10-lbm/sec design flow. The diffuser exit radius is 14.3 inches and can incorporate a diffuser of both vaned and vaneless types. The impeller consists of 15 blades and 15 splitters while the vaned diffuser has 24 two-dimensional wedge vanes. The stage has a design speed of approximately 21800 rev/min depending on ambient running conditions. The impeller is unshrouded and so incorporates a tip clearance. The tip clearance on this test rig can be varied so as to generate flow fields for varying tip clearances. The splitter blade is located at mid pitch and is identical to the main blade except that it has no inducer.

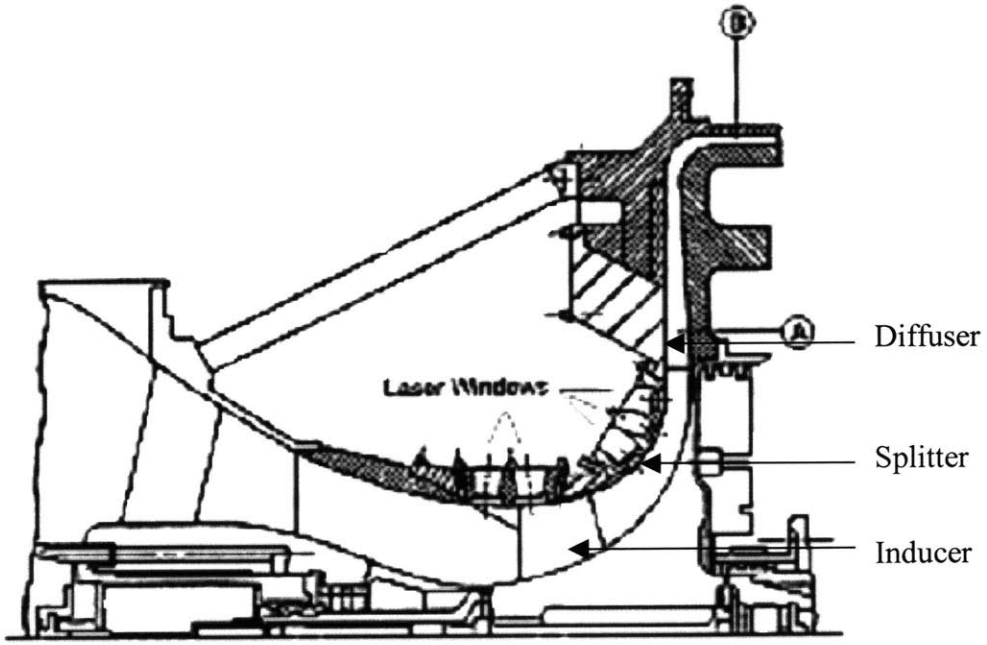

Figure 1-2 Model of NASA CC3 impeller/diffuser test rig.

The tip clearance is varied using an axial displacement shim. The axial movement of the stage in relation to the casing has the effect of producing an increasing tip clearance along the length of the blade. A picture of the impeller and diffuser is shown in figure 1-3.

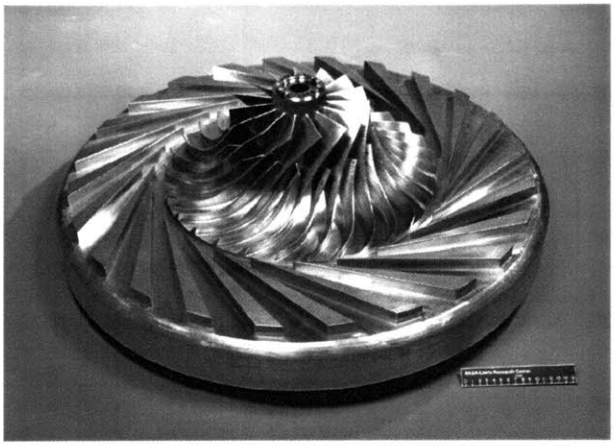

Figure1-3 NASA CC3 impeller/vaned diffuser stage. Courtesy of NASA Glenn Research Center.

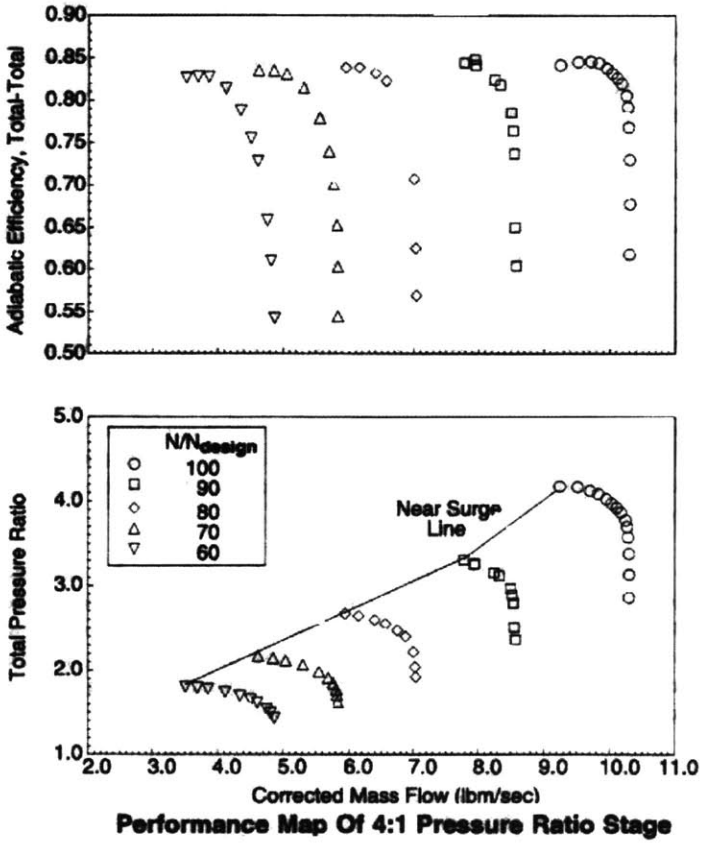

Figure 1-4 Performance map of NASA CC3 impeller/ 24 vaned diffuser test rig.

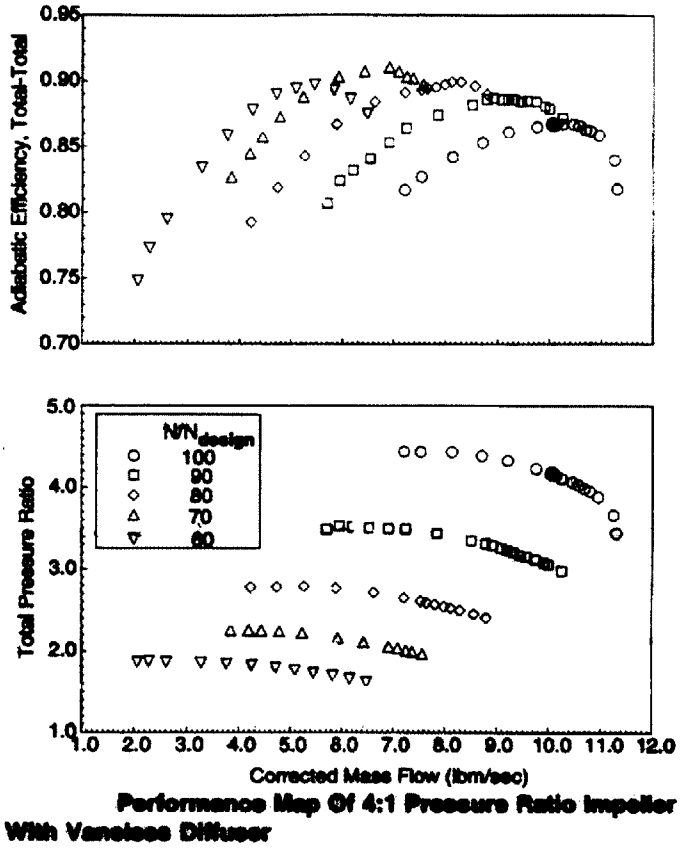

Figure 1-5 Performance map of NASA CC3 impeller/vaneless diffuser test rig.

Figures 1-4 and 1-5 show the performance curves for the NASA CC3 stage (taken from [23]) with vaned and vaneless diffusers respectively. The tip clearance in the impeller for these curves had a distribution of 0.1524mm (~0.2% of local blade span) at leading edge, 0.61mm (~1.4% of local blade span) at mid-chord and 0.203mm (~1.2% of local blade span) at trailing edge.

1.3 Previous Work

The availability of computer resources has revolutionized the work being undertaken in turbo-machinery fluid dynamics, by allowing for accurate three dimensional flow fields to be calculated. Much of this work is in progress and may not have been fully exploited as yet. However, research to date has led to useful results [17,18,21].

The importance of tip flow to the performance of the centrifugal compressor has been identified in many previous works. Brasz [3] concluded that tip clearance had a major effect on the overall output of a compressor stage. He demonstrates through his experimentation that the influence of tip clearance on overall performance metrics is non-linear and that performance sensitivity is higher at smaller tip clearances. It was argued that work input was responsible for this "non-linear effect". However, Brasz [3] does not identify an optimal tip clearance.

Previous works propose the existence of an optimal tip clearance that is greater than zero. This optimality is argued by Cumpsty [5] to be due to the interaction of the tip flow and secondary flow at the shroud suction surface. Senoo [19] however states that it is likely that the optimum is too small for practice. Senoo [20] argues that the presence of tip clearance alters the velocity distribution downstream and can affect the pressure recovery in the diffuser. He states that this change in distribution can be exploited by redesigning the geometry.

Shum [21] showed that an optimal impeller-diffuser gap could be determined using Dawes [6] *UNNEWT* code through assessing the performance trends of the centrifugal compressor stage with three different impeller-diffuser gap sizes. Shum [21] found that the impeller performance was not linearly dependent on the impeller-diffuser gap size. Instead he showed that there exists an optimal gap size where the impeller performance is at a maximum. Shum [21] linked this local maximum to the time-averaged change in slip, loss and blockage at the impeller exit associated with the unsteadiness generated by the vaned diffuser. He showed that decreasing the gap size can reduce blockage, decrease slip and increase loss. A one-dimensional (1D) model was

developed to show how these three parameters affected the overall performance. The CFD results from Shum's [21] work imply that the time-averaged change in performance occurs in the impeller; however negligible change in the performance is observed in the diffuser when changes in diffuser flow alignment are excluded. His explanation for the performance change relies on his surmise that the unsteady pressure field and its upstream influence effects the tip clearance flow and therefore the overall performance of the stage. Shum's [21] calculations included only one tip clearance and there is thus a need to determine the performance change for different impeller tip clearances in light of his model and results. Shum's [21] work does however show that unsteadiness can potentially be used to the designers' advantage. Moreover, his work demonstrates that further research is required to understand the processes behind unsteady interaction so that centrifugal compressor stages can be made more efficient.

Philips [18] showed on a computational basis that the dependence of diffuser pressure recovery on axial distortions was low when compared with the coupling between diffuser pressure recovery and inlet flow alignment. Philips [18] used the steady version of Dawes [6] three-dimensional Reynolds Averaged Navier-Stokes solver. He applied an inlet axial distortion to a diffuser geometry that was experimentally analyzed by Deniz [8]. His results compared well with Deniz's [8] rig results that showed the weak dependence of the diffuser recovery to inlet axial distortion. Both Philips [18] and Deniz [8] showed results that demonstrated the strong influence flow alignment has on pressure recovery. This is also verified by results found in chapter three of this thesis where the diffuser pressure recovery is found to be strongly linked to the flow alignment. Both Shum's [21] and Philips' [18] work demonstrated the adequacy of Dawes [6] code for computing unsteady three-dimensional flow in a centrifugal compressor stage near design.

1.4 Technical Objectives

The overall goal of this research is to quantity the effect of flow interaction between a downstream vaned diffuser and an upstream centrifugal impeller on performance. The specific technical objectives are:

(i) determine the effect of unsteadiness on impeller performance for an impeller with varying tip clearances.

(ii) identify the flow mechanisms responsible for the changes in performance of the impeller when a vaneless diffuser is replaced with a vaned diffuser.

(iii) identify the effect of diffuser blade count on the impeller performance and relate this to the findings of Shum [21].

To accomplish these objectives the following research questions must be addressed;

(i) How does changing the tip clearance or vane count influence the impeller-diffuser interaction and how does it impact compressor stage performance?

(ii) How does the presence of the downstream vanes affect the performance of the impeller?

In addition, it would also be valuable to establish whether the present computed results agree with the one-dimensional flow model as developed in [21].

1.5 Contributions

Key contributions from the present work are delineated in the following.

(1) *The change in performance of a centrifugal impeller due to a downstream vaned diffuser is dependent upon the tip clearance.*

While Shum [21] showed the dependence of the impeller performance on the radial gap, this thesis shows that the change in the performance of a centrifugal impeller due to a downstream vaned stator is dependent on the tip clearance. This means that it is important to know the exact running tip clearance of the impeller when designing the diffuser for optimum impeller efficiency.

(2) *A new phenomenon that affects the performance of the impeller has been identified for this specific centrifugal compressor stage. At design speed, tip flow back leakage can occur. This type of tip flow consists of tip flow that originates in one passage, flows downstream of the impeller trailing edge and then returns upstream of the impeller trailing edge into the casing region of a neighboring passage.*

(3) *Changing the radial gap distance between impeller and diffuser is analogous to changing the diffuser blade count.*

Chapter four of this thesis shows that a direct comparison between diffuser vane count and the radial gap can be made and that their influences on impeller performance are comparable. It is suggested that the ratio of impeller-diffuser gap to pitch of diffuser vane essentially characterizes their effect on impeller performance change.

(4) *New method of calculating the change in blockage in an impeller passage is proposed and developed.*

This thesis proposes and utilizes a new method of calculating the effect of a change in blockage on performance. Khalid's [17] method of blockage estimation was shown to be inappropriate for the impeller exit flow encountered here.

1.7 Thesis Outline

The thesis is organized as follows:

Chapter 2:

This chapter introduces and explains the technical and analytical tools used to conduct the analysis in subsequent chapters. Technical tools include the meshing and solver algorithms while analytical tools include the definition of blockage used in the analysis.

Chapter 3:

This chapter describes the results from computations in which the impeller tip clearance is varied for both vaned and vaneless stages. The results are compared to the trends found by Shum [21]. The tip flow back leakage phenomenon is introduced and shown to have an unsteady interaction with the downstream diffusers vanes.

Chapter 4:

This chapter describes the results from computations in which the vane count in the diffuser is varied for an upstream impeller with a tip clearance of 6%. The relationship between the results for which the diffuser vane count is varied and the results of Shum [21] for which the impeller-diffuser radial gap is varied is explored. Based on this a hypothesis on the effect of impeller-diffuser interaction is put forward.

Chapter 5:

The conclusions are presented along with a discussion pertaining to the success and overall achievements of this thesis. The relevance of identified phenomena is also discussed. Future work in the field is suggested in conjunction with justification thereof.

Chapter 2

Technical Approach

2.1 Introduction

This chapter steps through the research methodology from initial geometry modeling to flow field interpretation. Section 2.2 describes how the different flow fields are generated using computational fluid dynamics. Once an impeller-diffuser geometry has been defined with the appropriate boundary conditions imposed the associated flow field can be calculated. Section 2.3 delineates the set of seven calculations implemented to answer the two key research questions in this thesis, i.e. the effect of tip clearance on impeller performance and the effect of vane count on impeller performance in a centrifugal impeller-diffuser stage representative of modern design. Finally, 2.4 details procedures for post-processing the flow field into performance characteristics and flow specifics so that the cause and effect of the impeller-diffuser interaction can be established.

2.2 CFD Analysis

For many investigations involving fluid flows (especially in turbomachinery), measurement systems needed in experiments to resolve the flow field are often difficult to design and implement. Furthermore, measurement techniques may be such that neither flow details nor the change associated with introduction of flow disturbances and configuration alteration (such as tip clearance etc.) can be captured. Internal flow problems pose even greater difficulties. Accessibility is a major problem. Often measurement probes cannot be located at the place of interest. The advent of high speed computing has meant that other techniques can provide the needed capability. For fluid flow problems, use of Computational Fluid Dynamics (CFD), as a tool for implementing numerical experiments has led to useful technical results ([18] and [21] for example).

In this thesis, flows in centrifugal impeller-diffuser stages with varying tip clearances and diffuser vane counts are numerically simulated using CFD and analyzed to identify the cause and effect between unsteadiness due to impeller-diffuser interaction and the change in time-averaged performance. In order to do this, distributions of pressure, density and velocity in the flow field may be needed. CFD is used because it would be difficult (if not impossible) to obtain the required flow details in experiments. Sections 2.2.1 – 2.2.3 explain the computational tools used to generate a numerically simulated flow field that is deemed adequate for the purpose here.

2.2.1 Compressor Geometry

The centrifugal compressor geometry used in this thesis is the CC3 test stage in the test cell located in the Small Engine Components Test Facility (SECTF) at NASA Glenn Research Center, Cleveland, Ohio. The geometry is modeled using *UNNEWT Mesh*. This code was written by Professor W. Dawes from Cambridge University for use with his three dimensional Reynolds-averaged Navier-Stokes solver. It uses a Cartesian

coordinate system with the axial (X), tangential (T) and radial (R) coordinates (with index j, i, k to denote nodes in the respective direction) in the right-handed set. The code uses blocks to define the different geometries in the calculation and can appropriate different rotational speeds to each of these blocks to account for rotating and non-rotating parts. Shum [21] demonstrated the utility of this code for computing unsteady flow in centrifugal compressor stages.

The grid generation uses a H-mesh type with geometric stretching. The grid is then unstructured and cells that are flagged as not present are deleted. The code allows for mesh refinement to tailor for specific investigations. This refinement can be used to simulate cooling holes, increase fillets or radii and to increase mesh density at specific locations for resolution of required flow details. Advantages of this mesh generator include ease of data entry and symmetry of cells.

The overall stage is modeled by separating both the impeller and the diffuser into different blocks. The impeller block is given a rotation and initial inlet boundary condition while the diffuser is given a zero rotation and initial exit boundary condition. The resulting file (known as an mcv file) is used as the initial flow field for the CFD solver code. Figure 2-1 shows the resulting mesh for the impeller with 6% tip clearance and 30 vaned diffuser.

The density of the mesh was increased in the tip region relative to the main flow so that the tip flow field could be captured without wasting computational resources. The trailing edge region of vaneless diffusers was tapered to help convergence of the solution in the solver. This did not affect the results in the impeller-diffuser interaction region because the tapering started at a distance of one diffuser blade chord downstream of the impeller trailing edge. This method of geometry tapering was done in accordance with recommendations by Skoch [24].

The geometry of the diffusers vanes was altered to ease computational resources. The original vaned diffuser geometry in the NASA CC3 test rig has 24 vanes. It was necessary to scale the thickness of the blades so that vane counts of 30 and 15 could be used. Counts of 30 and 15 were chosen so that the impeller blade ratio (including splitter) to diffuser vane ratio was 1 and 2. Using these ratios allowed for calculations of low blade count to be run in the solver. The diffuser vane thickness was altered so that

the original flow area was conserved. This lowered the node number of the calculation and hence the solution time. This technique was decided upon following consultation with Skoch [24] and Tan [25].

In all cases, the geometry and mesh were built as identical as was possible so that any systematic error associated with the computation was similar for all cases; in this manner their effects could be minimized and thus neglected when making comparisons.

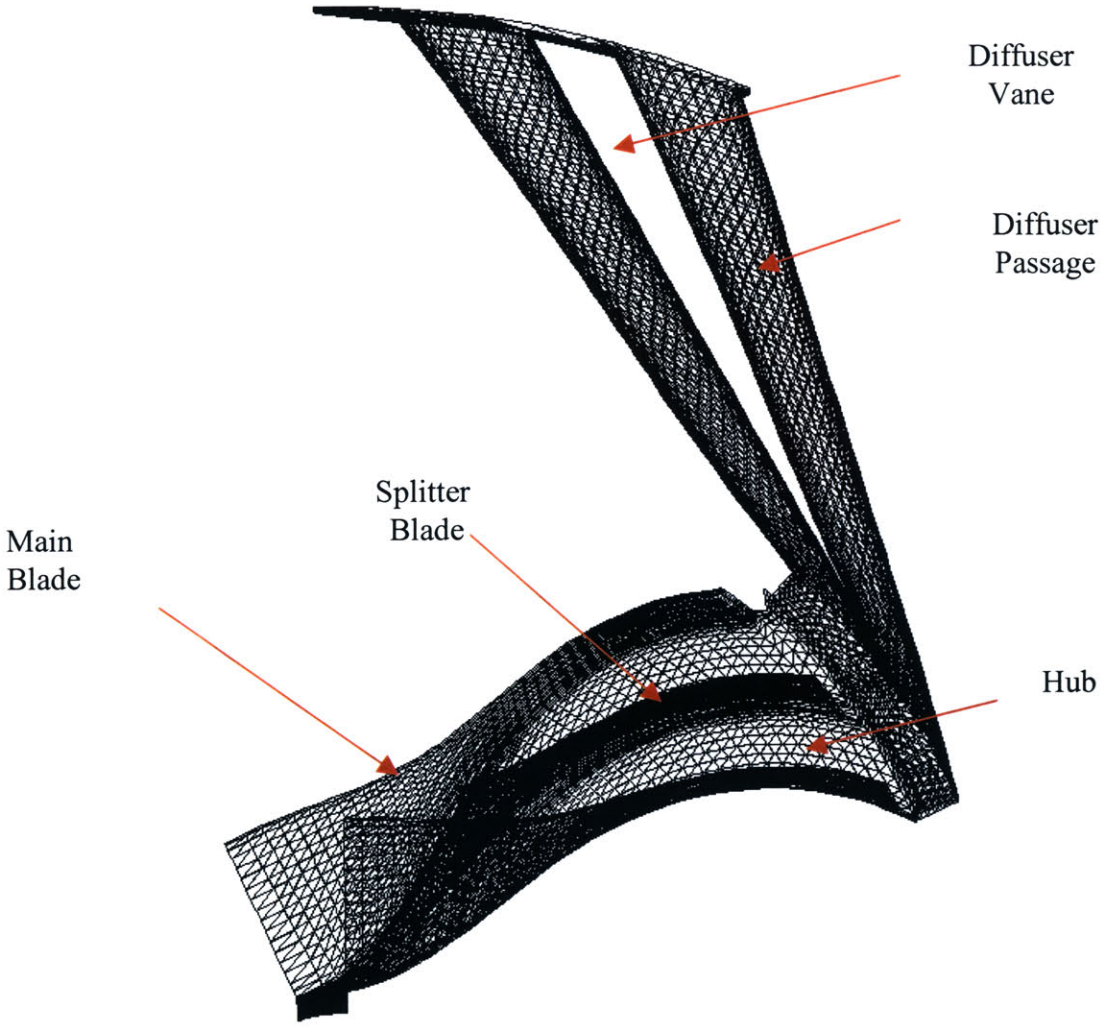

Figure 2-1 Mesh for 6% tip clearance impeller with 30 vaned diffuser.

2.2.2 CFD Solver

The CFD solver used is *UNNEWT*; Professor W. Dawes of Cambridge University developed it. It is an unstructured mesh, solution adaptive, fully three dimensional, compressible Navier-Stokes solver with sliding boundaries. The code uses a flow field calculated from a separate computer program based on a mesh generated as described in section 2.2.1 and a run file as inputs. This run file controls both initial and future calculations of the specific mesh.

The calculation was brought up to design speed using a load stepping procedure starting at 30% of design speed. When this solution had converged to a point where large transients in the flow field had decayed to a negligible level, the speed of the rotor and the back-pressure at the diffuser outlet plane were increased. This method was repeated until the flow field was at the design speed and the design corrected mass flow. Load stepping is necessary because the code is sensitive to large perturbations. The solver allows for load stepping in the run file with an adjustable number of previous steps. The output from the solver is dumped in an unstructured format and requires structuring for post-processing.

2.2.3 Visualization

Visualization for the output from the flow solver was essentially implemented with the use of *FIELDVIEW* [27]. *UNNEWT* dumps static pressure, density and velocity as outputs along with grid co-ordinates and connectivities. From these outputs various parameters such as blockage and entropy were computed. *FIELDVIEW* allowed for simple mesh and flow visualization and provided basic algebraic functions so that parameters such as total pressure could be calculated and visualized.

Figure 2-2 demonstrates the capabilities of the visualization by plotting the streamlines of the tip clearance flow. The expected tip vortex is depicted coming off the

blade tips of the main and splitter blade. A lower loading across the splitter blade produces a more localized tip vortex with a smaller core radius.

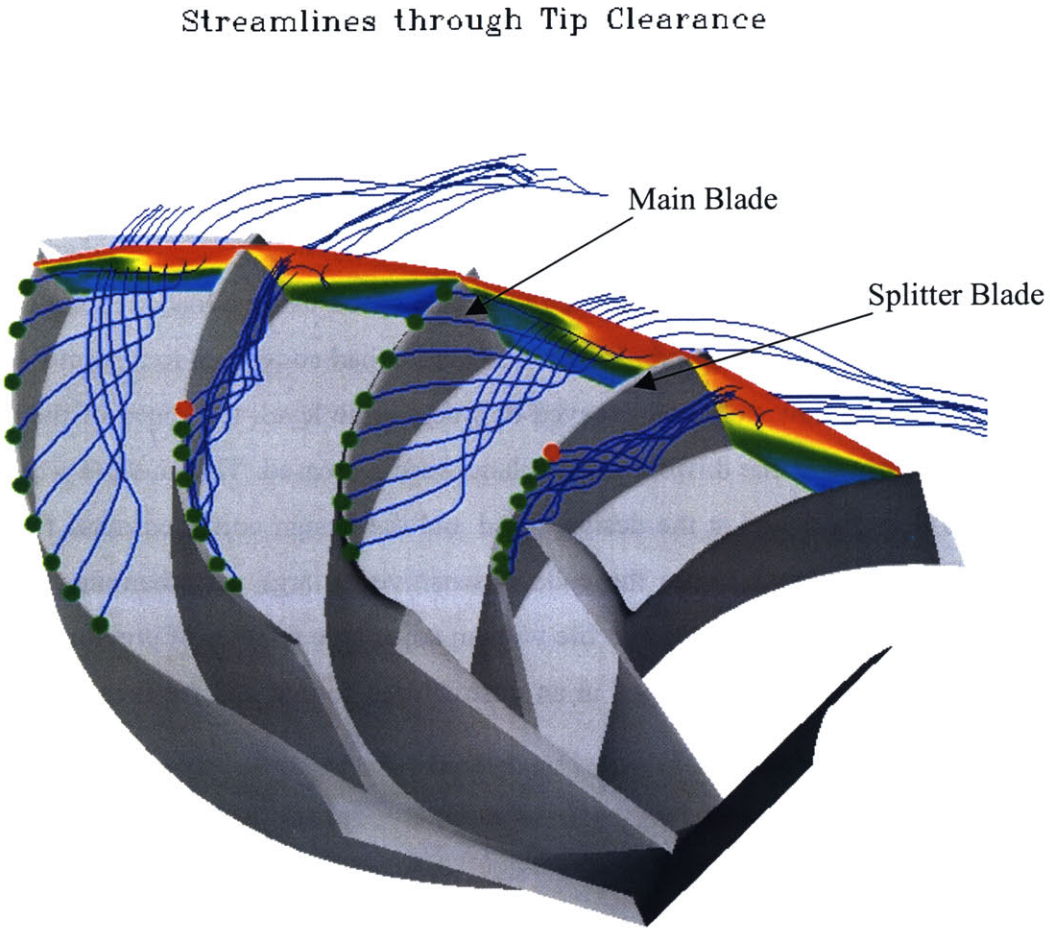

Figure 2-2 Streamlines of tip flow for vaneless diffuser, 6% tip clearance impeller.

2.3 Computations and Technical Framework of Approach

As mentioned in section 1.1, this thesis is focused on addressing two key technical questions. The first question that needs to be answered regards the effect of tip clearance on the unsteady interaction between the impeller and diffuser. Six different calculations were carried out in order to address this issue. These are described in table 2-1

Case Number	Number of Vanes	% Tip Clearance	Corrected Mass Flow +/- 1%
1	0	0	4.5 kg/s
2	0	4	4.5 kg/s
3	0	6	4.5 kg/s
4	30	0	4.5 kg/s
5	30	4	4.5 kg/s
6	30	6	4.5 kg/s

Table 2-1 Summary of calculations for assessing the effect of tip clearance variation on impeller performance.

Comparing case 3 and 6 allowed for the isolation of the effect of unsteadiness on the time-averaged performance of a 6% tip clearance impeller. The difference between case 3 and 6 lie in the diffuser geometry. Case 3 has a vaneless diffuser downstream while case 6 has a vaned diffuser with 30 vanes downstream. Using the data reduction techniques that will be described in section 2-4, a comparison between different performance metrics could be made between the two cases. This effectively isolated the time-averaged effect of placing a vaned diffuser downstream of the impeller. It can also be seen as increasing the impeller-diffuser interaction from zero as outlined in Shum [21].

Repeating the analysis performed at 6% tip clearance for two other tip clearances 0% and 4% isolated the dependence of this unsteady impeller-diffuser interaction on tip clearance. Calculations 1 & 4 were compared for the 0% tip clearance analysis and cases 2 & 5 were compared for the 4% tip clearance analysis. These results could then be used to answer the first question of the thesis, i.e. how does changing the tip clearance affect the time-averaged performance of the impeller. These computed flow fields could also be utilized to assess the effect of the unsteady impeller-diffuser interaction on the diffuser performance as was done for the impeller performance.

An additional calculation was implemented to address the second question of this thesis regarding the effect of diffuser vane count on impeller performance. This seventh calculation was used in conjunction with two of the previous cases to make the final statement on how the vane count affects the impeller performance. Table 2-2 summarizes the computations for assessing the effect of diffuser vane count. Comparing these three calculations enabled a statement to be made on the importance of diffuser blade count on the performance of the impeller by calculating the performance of the impeller for each of the three cases.

The calculations used to answer both research questions will be identified as cases 1 to 7 in the remainder of the thesis.

Case Number	Number of Vanes	% Tip Clearance	Corrected Mass Flow +/- 1%
3	0	6	4.5 kg/s
6	30	6	4.5 kg/s
7	15	6	4.5 kg/s

Table 2-2 Summary of calculations for assessing the effect of vane count variation on impeller performance.

2.4 Description of Performance Metrics

This section describes the procedures (geometrical complexity of centrifugal compressor flow paths pose some challenges in the development of these procedures) used to convert the flow field calculated using CFD into figures of merit that can be used to analyze the overall performance of the stage. Shum [21] determined that the unsteady interaction between the downstream diffuser and the upstream impeller changed the impeller performance through time-averaged changes in blockage, slip and entropy. Since the key focus here is on the unsteady impeller-diffuser interaction, the method for extracting these parameters from the computed flow field is described here.

2.4.1 Mass Averaging and Time Averaging

It is known that the flow exiting the impeller and entering the diffuser has a 'Jet and Wake' flow structure. The 'Jet' corresponds to the high speed, low-pressure flow at the suction side of the blade passage and the 'Wake' corresponds to the high pressure and low velocity pressure side flow. This analogy was first introduced by Dean *et al.* [7]. In view of the extent of the flow non-uniformity, it is appropriate to use a mass averaging technique to define properties of the flow.

The definition of mass averaged is given below where f is a flow variable such as total pressure:

$$f_{\text{mass-averaged}} = \frac{\int f.d\dot{m}}{\int \dot{m}}$$

Parameters such as total pressure can be mass averaged over a plane using the above definition, thus providing a single number for the total pressure at that plane.

A second complication that arises through this study is the fact that the calculations are unsteady. Therefore a second averaging technique must be used to take into account the fact that the flow has different properties at different time-steps. Time averaging is performed using the following definition where f(t) is the local value of a flow variable f at time-step N:

$$f_{\text{time-averaged}} = \frac{\sum_1^N f(t)}{N}$$

This definition assumes that the time-steps are equal, a condition that is met in here.

For all calculations the entire flow field was time averaged at each node before any other data analysis tools were used. This allowed for analysis to be done on one time-averaged flow field instead of a set of time dependent flow fields.

2.4.2 Blockage

Blockage is an important parameter in compressors as it controls the amount of pressure recovery achievable in the blade passage. If the blockage increases, the effective area decreases leading to an increase in the local velocity and decrease in the local static pressure, thus, less pressure recovery is possible. Aknouche [1] showed that less than 100% of this static pressure drop is recovered in the diffuser. Shum [21] showed that not only is blockage important to static pressure recovery but it is also an important factor when isolating the affect of unsteadiness on stage efficiency for centrifugal compressor stages.

Blockage occurs when momentum defects develop in a blade passage. Many authors have shown that tip flows increase the blockage of a blade passage through the introduction of momentum defects [1, 16, 17, 21]. In centrifugal compressors the region of momentum defect is not readily identifiable from the main flow and so the calculation of blockage is difficult.

While in external flows the main flow is readily determined because it is the region of uniform flow, it is more complex in situations involving the main or free-stream flow in a rotating passage because the presence of a relative eddy would generate a varying free-stream velocity. There are a number of different methods of addressing the problem of identifying the free-stream. The method used by Shum [21] for calculating blockage is an adaptation of Khalid's [17] method for axial compressors. Essentially, it is the same method but differs in the details of the implementation for centrifugal compressors. This will be further elaborated on in section 2.4.2.2.

The next section defines blockage, describes Shum's adaptation of Khalid's method and the difficulties encountered in its application in the current investigation. A new method that overcomes the difficulties encountered is proposed.

2.4.2.1 General Definition of Blockage

The blockage of a blade passage cross-section is defined below in equation 2.1.

$$B = 1 - \frac{A_{eff}}{A_{act}} \tag{2.1}$$

In equation 2.1 A_{eff} is the effective area of the passage when blockage is taken into account and A_{act} is the actual geometric area of the passage. The blocked area, A_B as given in equation 2.2 below, is analogous to the displacement thickness as applied to boundary layers.

$$A_B = B.A_{act} \tag{2.2}$$

The displacement thickness (δ) of a boundary layer is demonstrated in figure 2-3 and is explained in detail in references [2, 9].

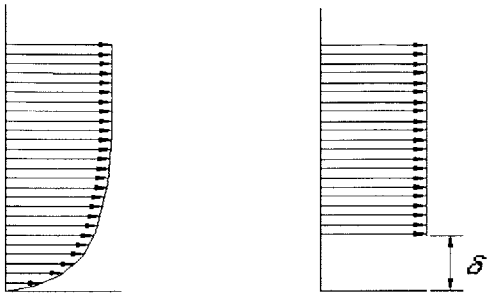

Figure 2-3 Boundary layer and displacement thickness.

The reduction in effective area due to the flow blockage generation results in a reduction of pressure rise capability.

This section described the definition of blockage as is used and how it can have an affect on the pressure rise capability of fluid devices. Using this definition as a basis, a more specific definition can be used to determine the blockage of rotating flows as encountered in centrifugal impeller passages. The following sections describe Khalid's/ Shum's procedure of calculating blockage and the alternative procedure adopted here.

2.4.2.2 Khalid's/Shum's Method

Khalid's [17] expression for the blocked area is given as;

$$A_B = \int \left(1 - \frac{\rho V_{TF}}{\rho_e V_e}\right) dA \tag{2.5}$$

where $B = \frac{A_B}{A_{act}}$

To calculate the value for $\rho_e V_e$, Khalid [17] acknowledged that the magnitudes of the gradient of $\rho\vec{V}$ are much higher in the defect area than in the core flow. Calculating the gradient for the components of $\rho\vec{V}$ orthogonal to the main flow vector gives an indication of the extent of the core flow. Khalid [17] identified this core region, as being the region, whose gradient normalized by $\frac{\rho_{av} V_x}{c}$, was less than 2. The region where $\frac{\rho_{av} V_x}{c}$ was equal to 2 was defined as the cutoff region. The values of $\rho\vec{V}$ on this cutoff region determine the values of $\rho_e V_e$. Shum[21] redefined the normalization to be $\frac{\rho_{av} W_{av}}{D}$ to account for the differences between axial and centrifugal compressors. To illustrate this approach, Figure 2-4 shows a plot of the normalized magnitude of the gradient of $(\rho\vec{V})_\perp$ for a plane upstream of the blade leading edge of a centrifugal impeller. The circumferential regions of high $\left|\nabla(\rho\vec{V})\right|$ are located adjacent to the passage hub and tip corresponding to the boundary layers.

Using Khalid's/Shum's method, a cutoff region would be specified visually and a number for blockage would be calculated using the above definition. In Figure 2-4 the region of mass flux defect is easily located visually in the boundary layers at hub and shroud, however, Khalid [17] describes how verifying the location of the mass flux defect in an axial machine is not as straightforward. Figure 2-5 is a figure from Khalid [17] that shows the region that Khalid [17] specified as his defect region. In this diagram, Khalid [17]demonstrates how some areas of low mass flux gradient had to be included in the defect region. The reasoning behind this was that even though these regions do not fulfill the requirements of high mass flux gradient, they are clearly lying in the area that is affected by the mass flux defect. Not including these regions in the blocked area would lead to inaccurate estimations of blockage.

This problem becomes even more complicated in centrifugal machinery as can be seen from figure 2-6. This figure shows the mass flux gradient at the CC3 impeller exit. In this case the exact regions of blocked area are not obvious from the contours of mass

flux gradient. Khalid's/Shum's method requires a visual estimation of the blocked area. The author decided that such estimation could not be relied upon for a reliable and acceptable method of determining changes in performance of centrifugal compressors. For this reason an alternative method for calculating blockage is proposed. This alternative method is described in section 2.4.2.3 and does not rely on such estimations.

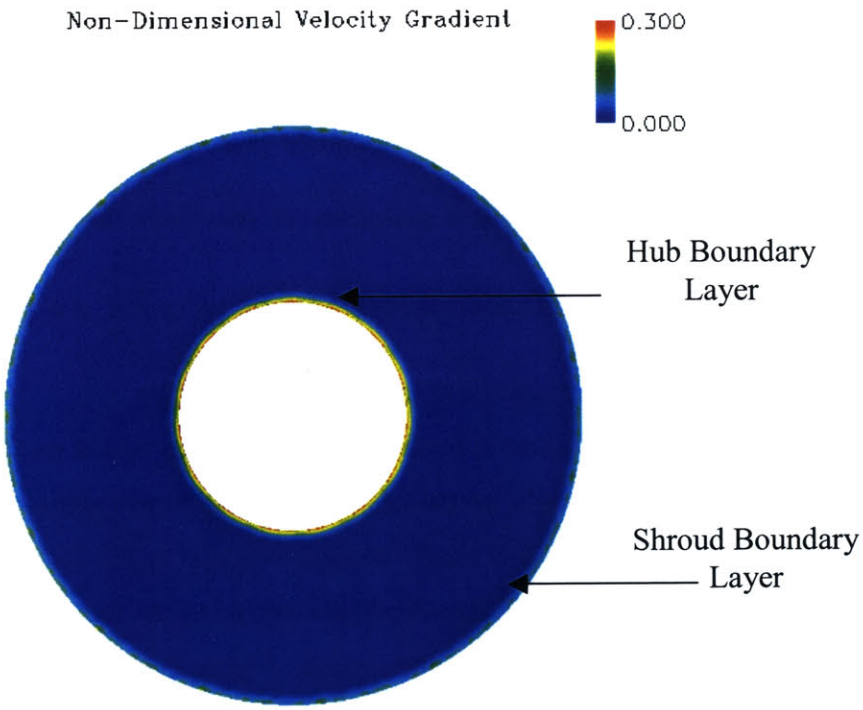

Figure 2-4 Values of $|\nabla(\rho V)|$ upstream of an impeller stage showing increased mass flux gradient in boundary layers.

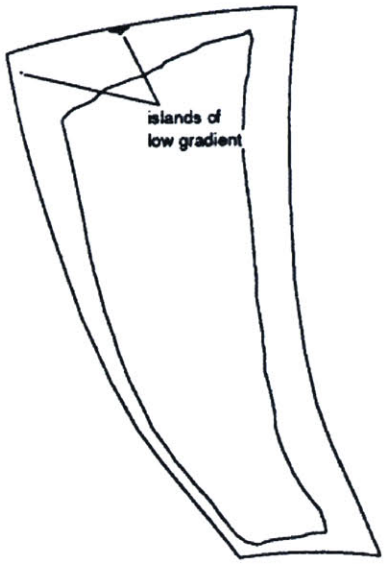

Figure 2-5 Gradient region from Khalid [17].

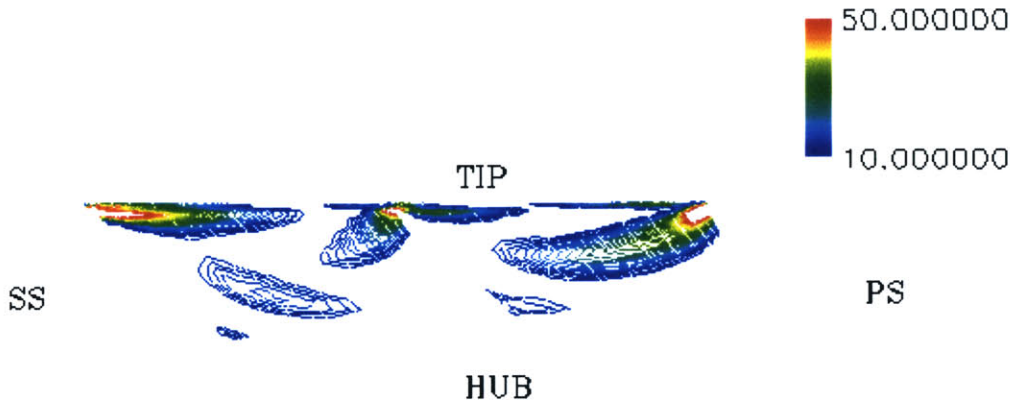

Figure 2-6 The value of $\left|\nabla(\rho W)\right|$ normalized by $\frac{\rho_{av} W_{av}}{r_2}$ at trailing edge plane of 6% tip clearance case.

2.4.2.3 Alternative Method for Estimating Change in Flow Blockage

While an absolute value for blockage is convenient, it is not absolutely necessary. This section demonstrates how the value for the change in blockage suffices for the purpose here.

Shum [21] developed a one-dimensional model for the change in total pressure to isolate the respective effects of blockage, entropy and slip on the total pressure of an impeller. The details for the development of the one-dimensional model are in reference [21]. For here, the final equations relating the change in total pressure to the change in blockage, entropy and slip are given below. C_A, C_S and C_θ are influence coefficients of area (blockage), entropy and slip respectively

$$\frac{\Delta Pt}{Pt} = C_A\left(\frac{\Delta A_{eff}}{A_{eff}}\right) + C_S\left(\frac{\Delta s}{Cp}\right) + C_\theta\left(-\Delta\theta\right) \tag{2.6}$$

$$C_A = \left(\frac{U - V_t}{V_t}\right)\left(\frac{1}{1 - M_{rel}{}^2}\right)\left(\frac{\gamma}{\gamma - 1}\right)\left(\frac{V_t U}{CpTt_1 + V_t U}\right) \tag{2.7}$$

$$C_S = -\left(1 + C_A\right)\left(\frac{\gamma}{\gamma - 1}\right) \tag{2.8}$$

$$C_\theta = \left(\frac{1}{\tan\alpha}\right)\left(\frac{\gamma}{\gamma - 1}\right)\left(\frac{V_t U}{CpTt_1 + V_t U}\right) \tag{2.9}$$

In equation 2.6 to 2.9 a relationship for the change in effective area is used in place of blockage. If it is assumed that there is a mean flow direction and that any deviation from this mean flow (through flow) direction will produce blockage, then, we can compare two similar flow fields and isolate the change in the deviation from the mean flow direction. Returning to the definition of blockage it can be noted that only the

component of mass flux that is in the mean flow direction contributes to the change in effective flow area. All other components of the mass flux vector contribute to blockage. Thus the change in effective area can be calculated as:

$$\Delta A_{eff} = \Delta\left(\frac{\overset{\circ}{m}.\int d\overset{\circ}{m}}{\int \rho W_{TF}.d\overset{\circ}{m}}\right) \tag{2.10}$$

where $\overset{\circ}{m}$ is the mass flow rate and W_{TF} is the relative velocity in the through flow direction.

This equation can therefore be used to isolate a value for the change in blockage between two similar flow fields. This number can then be used in conjunction with Shum's [21] one-dimensional model to identify the effect of blockage on the impeller performance. Equation 2.10 can be evaluated without visual or approximation errors. This is important because the isolation of small changes in performance can only be done if errors are limited.

2.4.3 Entropy and Slip

The equations used to calculate entropy and slip are relatively straightforward. Entropy is defined by Shum [21] as:

$$(s_2 - s_1) = -R.\ln\left[\frac{Pt_2}{Pt_1}\Big/\left(\frac{Cp.Tt_1 + V_{t2}U_2}{Cp.Tt_1}\right)^{\frac{\gamma}{\gamma-1}}\right] \tag{2.11}$$

In contrast to blockage, slip can readily be calculated from the computed flow field. Since the slip angle depends upon both the radial velocity and relative tangential velocity (which in turn depends on the absolute tangential velocity), it can be shown that the change in the slip velocity between two identical geometries can be evaluated from the change in α. This can be seen more clearly in the velocity triangle in figure 2-7. If the absolute tangential velocity decreases the relative tangential velocity will increase and vice versa (this assumes that the rotational speed of the impeller is held constant). In this figure the slip angle is the angle between the relative velocity and the ideal relative velocity. The ideal relative velocity is the relative velocity of the flow that corresponds to the hypothetical situation where no slip occurred.

The change in slip ($\Delta\theta$) can therefore be equated to the change in α as follows:

$$\Delta\theta = -\Delta\alpha \tag{2.12}$$

α can be readily calculated from the computed flow field. The change in slip can be given as:

$$\Delta\theta = \Delta\left(\tan^{-1}\left(\frac{V_t}{V_r}\right)\right) \tag{2.13}$$

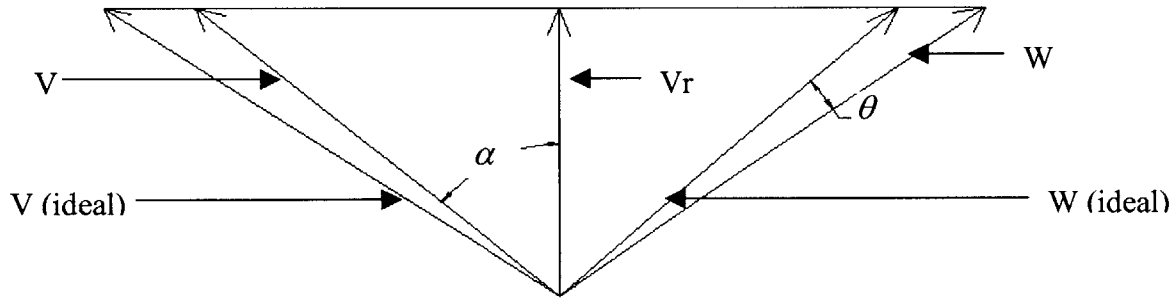

Figure 2-7 Velocity triangle for trailing edge of centrifugal impeller demonstrating the absolute flow angle and the slip angle.

2.4.4 Evaluation of Blockage, Entropy and Slip Metrics

Before we proceed to use the above-described procedures to post-process the computed results, we first apply them to Shum's one-dimensional model to determine the change in total pressure between case 3 and 6 (impeller-vaneless diffuser versus impeller vaned diffuser). This involves calculating the change in non-dimensional total pressure (based on absolute inlet dynamic head) using the change in blockage, change in entropy and change in slip angle from the computed flow fields of cases 3 and 6. This result for change in non-dimensional total pressure is assessed against the actual change in non-dimensional total pressure computed using CFD results. The values computed using these two methods are shown in figure 2-8 and they are in agreement.

The comparison validates the parameters used in the one-dimensional model and implies that statements on how blockage, entropy, slip and implicitly the performance of the stage are affected by changing the tip clearance and diffuser vane count can be made.

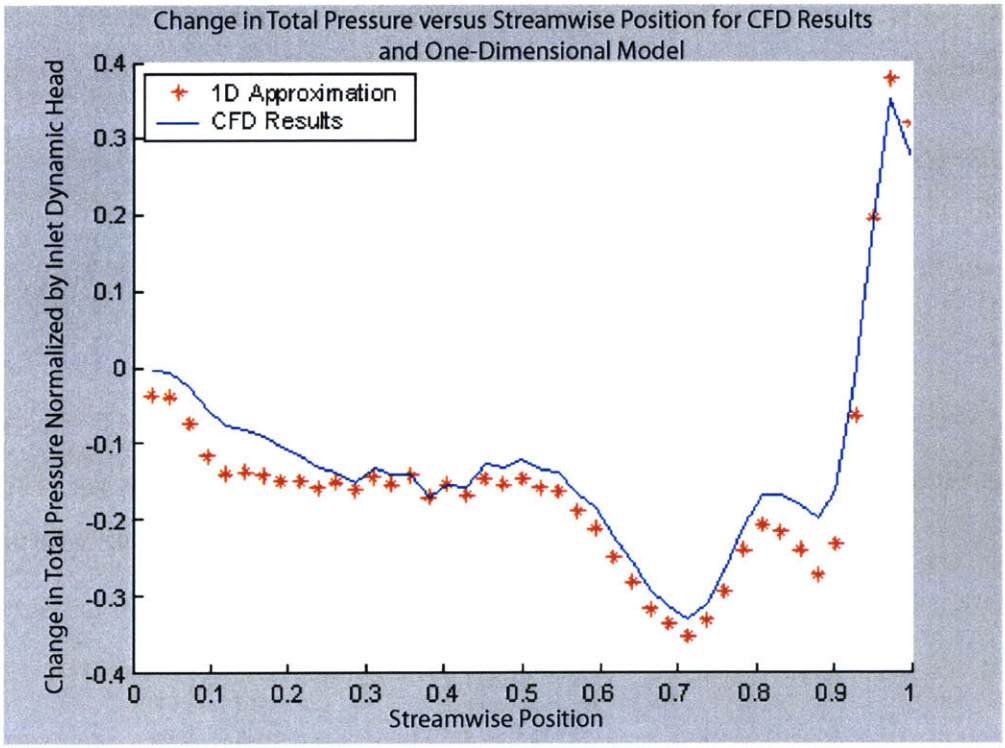

Figure 2-8 Comparison of change in total pressure due to the unsteady interaction as calculated by the one-dimensional model and CFD results. The ratio of absolute inlet dynamic head to $\frac{1}{2}\rho U^2$ is 10.6.

2.5 Summary

This chapter described the research methodology that will be used to answer the key research questions posed in section 1.1. Computing unsteady three-dimensional flow in a centrifugal impeller-diffuser stage using CFD was described and the ability of the selected CFD code [6] to capture the required flow details was demonstrated.

It was shown in section 2.3 that seven calculations in total are required to answer the two key research questions posed in section 1.1. The seven calculations consist of compressor configurations in which the impeller tip clearance and the diffuser vane count is varied.

A procedure is proposed and developed for isolating impeller passage blockage change without the need to define the region of blockage generation (which may incur a certain degree of arbitrariness). This method has been assessed for its applicability and utility.

Chapter 3

Effect of Impeller Tip Clearance Variation on Impeller and Diffuser Performance

3.1 Introduction

This chapter deals with the first research question posed in chapter 1. Specifically, it deals with the dependence of the performance of a centrifugal impeller-diffuser stage configured with vaned and vaneless diffusers on the impeller tip clearance. Sections 3-2 to 3-4 focus on the affect of the interaction on the impeller performance while section 3-5 focuses on the affect on the diffuser performance.

The global results for the impeller performance calculated in the study are presented in section 3-2. Three different tip clearances are compared (0, 4 & 6% of local span) using both vaned and vaneless diffusers downstream of the impeller. The relative performances between impellers with vaned and vaneless downstream diffusers are compared over the range of tip clearances to isolate the time-averaged impact of flow unsteadiness on the impeller performance. The dependence of the relative performance between vaned and vaneless diffusers on tip clearance is delineated and the existence of a tip clearance for optimal performance is deduced.

Section 3-3 isolates the parameters that drive the change in impeller performance between vaned and vaneless stages. The change in performance of an impeller is shown to be driven by the unsteady response of impeller tip flow. The flow unsteadiness

effectively changes the time-averaged value of entropy generation, blockage and slip, resulting in the change in performance as explained and discussed by Shum in [21].

Section 3-4 describes the trends of the influence coefficients with tip clearance variation. All the influence coefficients are found to depend non-monotonically on tip clearance.

Section 3-5 deals with the effect of the interaction on the diffuser performance. The performance is found to depend predominantly on the flow alignment with the diffuser vanes.

3.2 Global Performance Results of Impeller

The performances of each of the six configurations that have been calculated as part of this study to elucidate quantitatively the effects of tip clearance on performance changes are given in table 3-1. It is evident from the table that introducing a downstream vaned diffuser improves the total pressure ratio for all tip clearance configurations investigated.

Performances in Tip Clearance Variation Study (Mass flow =4.5 kg/s +/- 1%)					
Case No.	Vane No.	Tip Clearance	Total Pressure Ratio	Tangential Velocity (Normalized by U_2)	Polytropic Efficiency
1	0	0%	4.86	0.741	95.13%
2	30	0%	4.87	0.743	95.06%
3	0	4%	4.24	0.708	90.13%
4	30	4%	4.31	0.713	90.77%
5	0	6%	3.88	0.678	87.52%
6	30	6%	3.92	0.684	87.72%

Table 3-1 Summary of computed performances for centrifugal compressor stage with varying impeller tip clearance.

Figure 3-1 shows the relationship between the total pressure ratio and the tip clearance of the impeller for both the vaned and vaneless diffuser stages. The trend for total pressure

ratio shows that there is a tip clearance where the difference between the impeller total pressure ratio for vaned and vaneless diffuser stages is a maximum. This can be seen more clearly in figure 3-2 where the difference between the two stages has been extrapolated. Figure 3-2 indicates that at 0% tip clearance the difference between the total pressure ratios of the vaned and vaneless cases is small enough to be neglected (~0.004). The actual difference in total pressure ratio can be attributed to the fact that there exists a small discrepancy (<1%) between their mass flows.

If it is assumed that the total pressure ratios at 0% tip clearance are not affected by the type of downstream diffuser (as argued in the previous paragraph), it can also be argued that the total pressure ratio difference produced by the downstream vanes is a direct result of the interaction between the tip flow and the unsteady downstream pressure field. This is in agreement with Shum's [21] hypothesis and leads to two important implications. Firstly it is important to note that if this assumption is correct then designs of shrouded impeller stages will not have to take into account the unsteady interaction between impeller and diffuser when calculating the total pressure ratio through the impeller. Secondly, any design of an unshrouded impeller must address the issue of optimization when a downstream vaned diffuser is included. If this issue is not addressed then the performance of the impeller could be unnecessarily diminished. This will be shown to be so throughout this chapter and is in fact true whether or not the assumption made at the beginning of this paragraph is accurate or not.

The results for efficiency show similar trends to those for total pressure ratio. These are shown in figure 3-3. It is useful here to extract the change in efficiency between the vaned and vaneless cases at constant tip clearances. This is shown in figure 3-4. The efficiency for the vaned case is higher than that of the vaneless case except at low tip clearances. In this region the efficiency drops when the vane is introduced because the difference in total pressure ratio between the two is small compared to the increase in work done by the impeller when the vaned diffuser is introduced. Shum's [21] results at 2% impeller tip clearance are shown on the plot in figure 3-4. It should be noted that the interaction that Shum defined in [21] as medium and that corresponded to a ratio of the diffuser leading edge radius to impeller trailing edge radius of 1.092, is

consistent with the results from this study. The results in chapter four will show that 30 vanes in this study are comparable to "medium" interaction in Shum's study.

Similar to the total pressure ratio, the efficiency plot in figure 3-4 shows a strong indication that an optimal performance change exists. However, near 0% tip clearance the efficiency of the impeller with vaned diffuser can be less than that of the impeller with vaneless diffuser. Thus, in order for centrifugal compressors to be designed for limited losses by minimizing the tip clearance, it is necessary to have an accurate knowledge of the running tip clearance.

To illustrate this concept it is useful to take a hypothetical borderline case. Assume a case where a centrifugal compressor with vaned diffuser is being designed to optimize the impeller efficiency and say that the NASA-CC3 impeller-diffuser geometry is used. Suppose that for structural reasons a tip clearance needs to be included in the impeller design and designers decide to machine this tip clearance to 1% of the local span so that rubbing between the blade tip and impeller casing will not be a problem. If figures 3-1 to 3-4 are used as reference by the designers, then at one percent tip clearance, designers see that the presence of the diffuser coupled with the tip clearance improves the impeller performance. However, if during running conditions the actual tip clearance decreases to 0.2%, then the presence of the downstream vane coupled with the tip clearance actually decreases the efficiency. If designers had taken the running tip clearance into account instead of the "cold" unstressed tip clearance, steps could have been taken to reduce this negative effect such as designing the diffuser so that its upstream influence does not reach the impeller trailing edge. This is an important implication to future designs of centrifugal compressors with impeller-diffuser interactions.

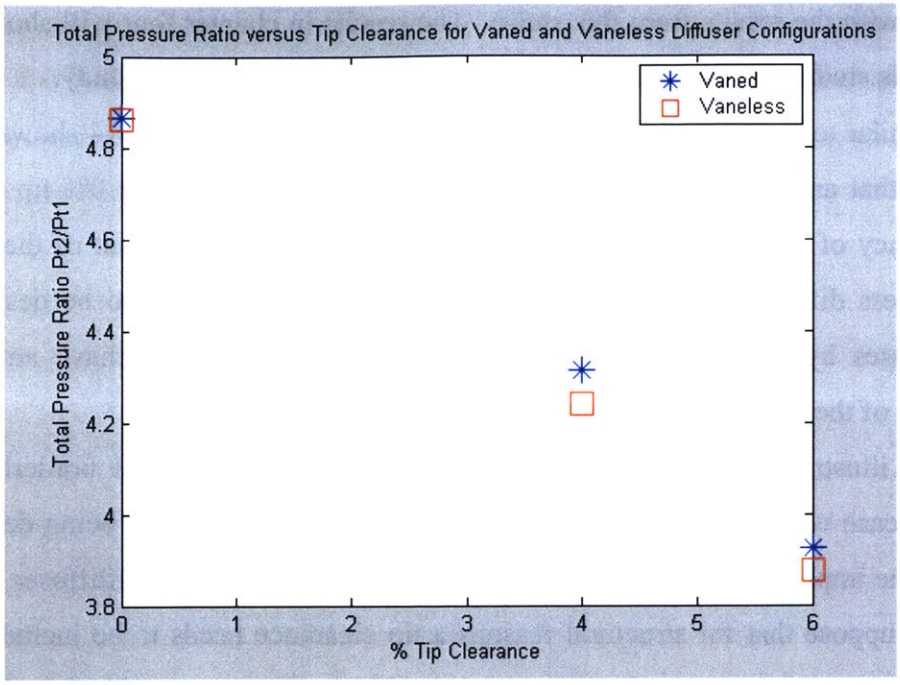

Figure 3-1 Computed trend in impeller total pressure ratio for vaned and vaneless configurations with impeller tip clearance variation to show the effect of downstream diffuser type on the impeller total pressure ratio.

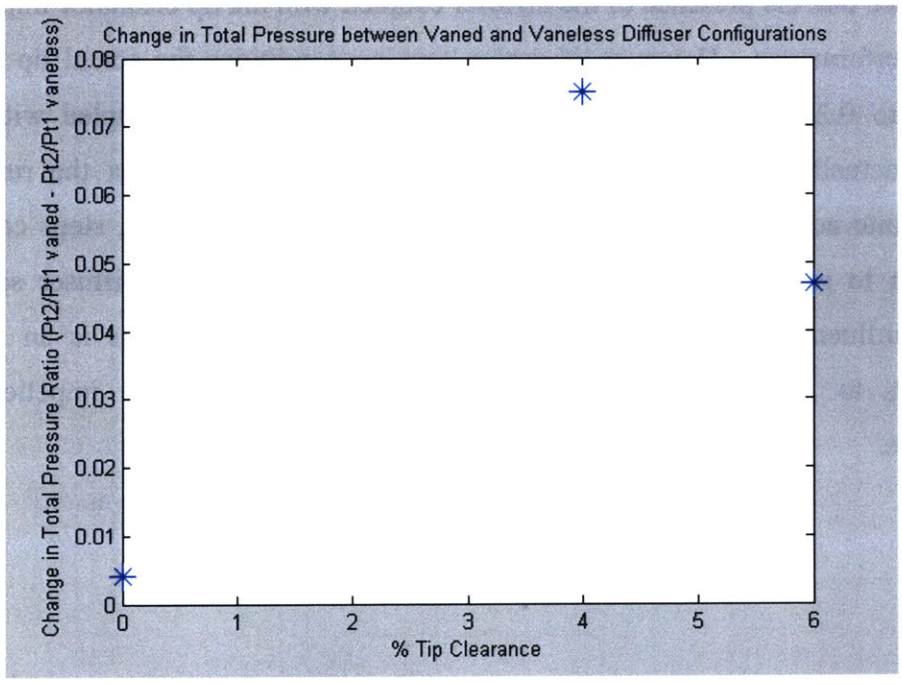

Figure 3-2 Change in the difference in total pressure ratio for impeller-vaned diffuser stage and impeller vaneless diffuser stage with impeller tip clearance variation to elucidate the non-monotonic trend.

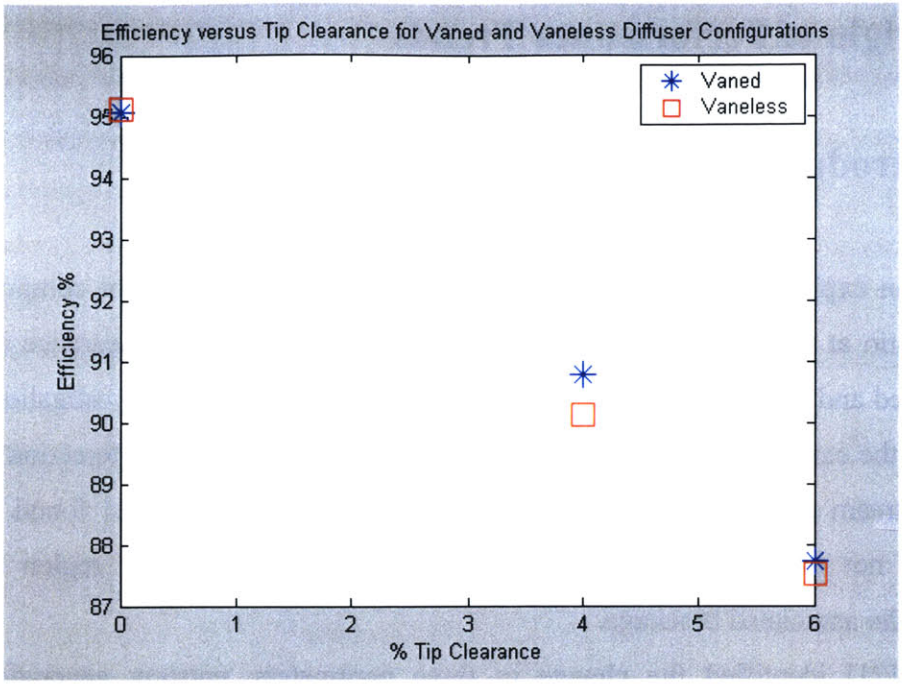

Figure 3-3 Computed trend in impeller efficiency for vaned and vaneless configurations with impeller tip clearance variation to show the effect of downstream diffuser type on the impeller total pressure ratio.

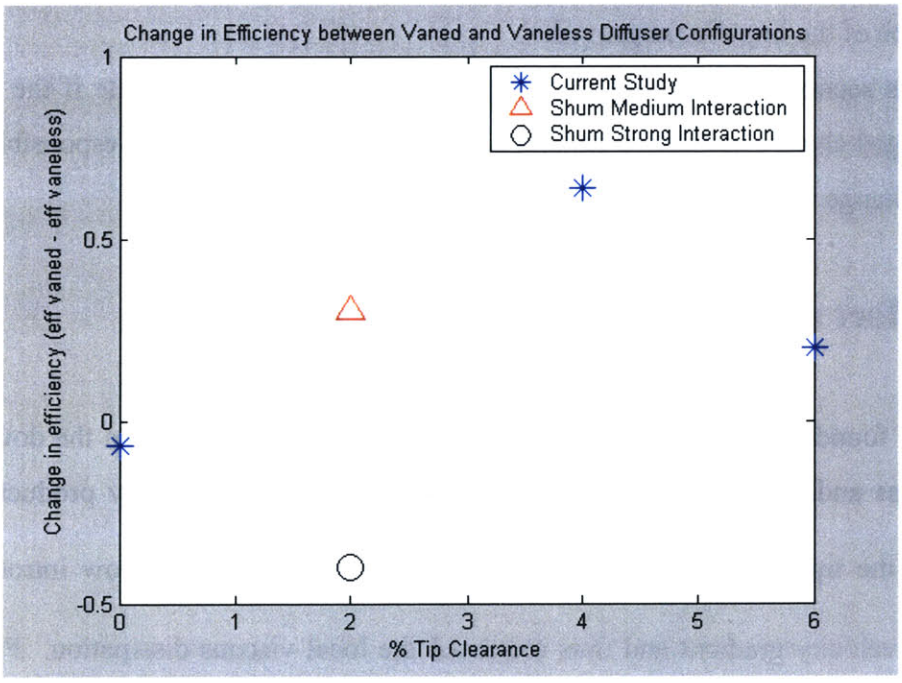

Figure 3-4 Change in the difference in efficiency for impeller-vaned diffuser stage and impeller vaneless diffuser stage with impeller tip clearance variation to elucidate the non-monotonic trend; computed results from Shum in [21] are shown for comparison.

3.3 Origin of Performance Trends

3.3.1 Introduction

This section explains the flow processes responsible for the change in computed total pressure ratio at the trailing edge plane between the 6% & 4% tip clearance impellers with a vaned and vaneless diffuser. Shum [21] conducted a similar investigation and he found that the cause of the change of performance was the unsteady interaction between the downstream diffuser and impeller tip clearance flow. Shum [21] found that this interaction not only increased entropy production in the tip flow region but also decreased the associated blockage.

Shum [21] identified the change in three parameters, entropy generation, flow blockage and slip angle as responsible for the change in performance. Shum [21] stated that if the overall increase in performance due to the change in blockage and slip was higher than the loss of performance due to an increase in entropy, the overall performance of the impeller improved.

This section will use the same approach as Shum [21] to isolate if the resulting time-averaged change in entropy generation, flow blockage and slip is responsible for the observed change in performance.

3.3.2 Effect of Interaction on Entropy Change

Shum [21] found in his research that increasing the interaction between the downstream unsteadiness and the upstream rotor increased the volumetric entropy production rate, $\rho\frac{Ds}{Dt}$, in the tip flow region. He reasoned that the unsteady tip flow introduced an additional velocity gradient and thus increased the local viscous dissipation. Figure 3.5 shows contours of $\rho\frac{Ds}{Dt}$ for the impeller with 6% tip clearance and a vaneless diffuser. Regions of high entropy production rate exist in three main regions.

The first region of high entropy production is at the blade boundary layer regions. High velocity gradients produced by the no-slip condition are responsible for this entropy generation. The second region of high entropy production is in the tip flow regions; these are highlighted in figure 3-5. The entropy production is greatest in the tip flow of the main blade because the loading at this blade is higher than on the splitter blade (the ratio of the loading on the main blade to that on the splitter blade of the impeller with 6% tip clearance at the 99% radius is approximately 1.85). This results in a tip vortex that encompasses more of the passage.

The final region of entropy production is produced by tip flow back leakage as will be elaborated on later. This phenomenon was observed at near stall conditions by Vo [26]. Such phenomenon is observed for the situation here at design speed and as can be seen in figure 3-5, generates a significant amount of entropy production. Though explained in more detail later this phenomenon must be recognized as a significant flow feature of engineering interest.

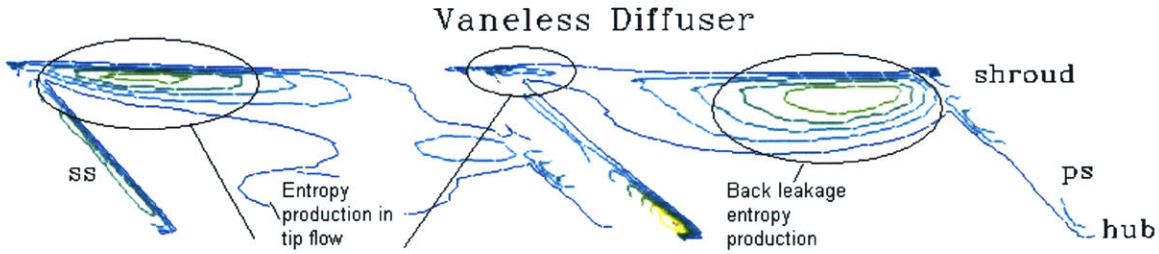

Figure 3-5 Contours of local entropy production rate at impeller trailing edge plane for vaneless diffuser case with 6% tip clearance in impeller showing areas of entropy production.

Similar to Shum's findings, the results in this research show local unsteadiness in the tip region. This can be observed from figures 3.6 to 3.10 where the contours of local rate of entropy production (normalized by $Tt_1/(\rho_1 V_\Delta t)$ are shown for the splitter blade for

five equal time steps over a blade passing in the vaned diffuser case with 6% impeller tip clearance. These plots could have also been shown for the main blade tip region, however, the nature of the post-processing in this investigation meant that the splitter blade tip region was more visually striking.

The values for local entropy production located closest to the splitter blade in figures 3-6 to 3-10 are plotted in figure 3-11 over time. These fluctuations show that the entropy production in the tip is unsteady.

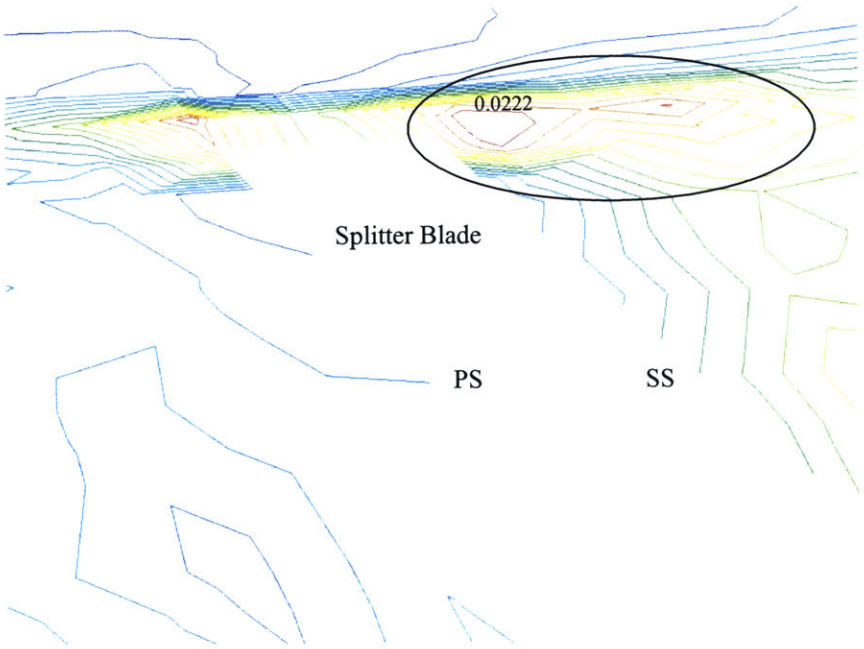

Figure 3-6 Contours of local entropy production rate at splitter normalized by $Tt_1/(\rho_1 V_\Delta t_{BP})$ for vaned diffuser and 6% tip clearance with the value of maximum contour at blade tip indicated -Time step 1.

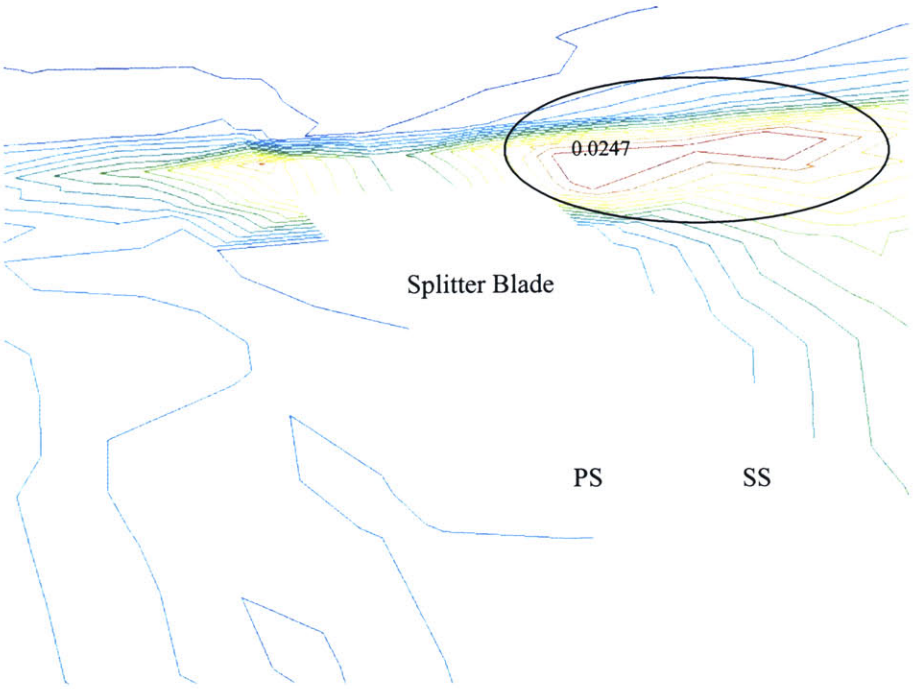

Figure 3-7 Contours of local entropy production rate at splitter normalized by $Tt_1/(\rho_1 V_\Delta t_{BP})$ for vaned diffuser and 6% tip clearance with the value of maximum contour at blade tip indicated -Time step 2.

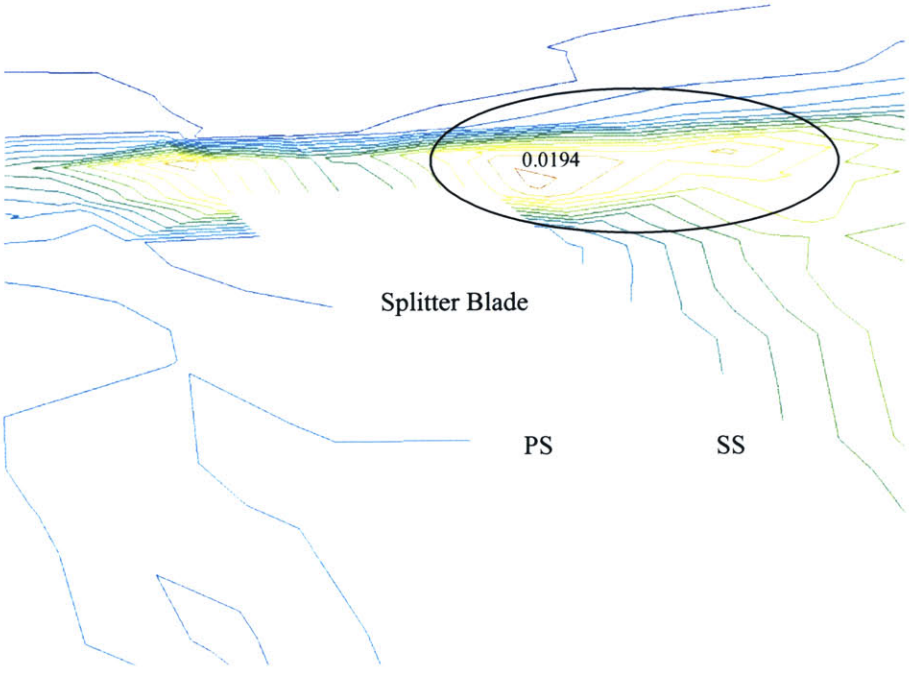

Figure 3-8 Contours of local entropy production rate at splitter normalized by $Tt_1/(\rho_1 V_\Delta t_{BP})$ for vaned diffuser and 6% tip clearance with the value of maximum contour at blade tip indicated -Time step 3.

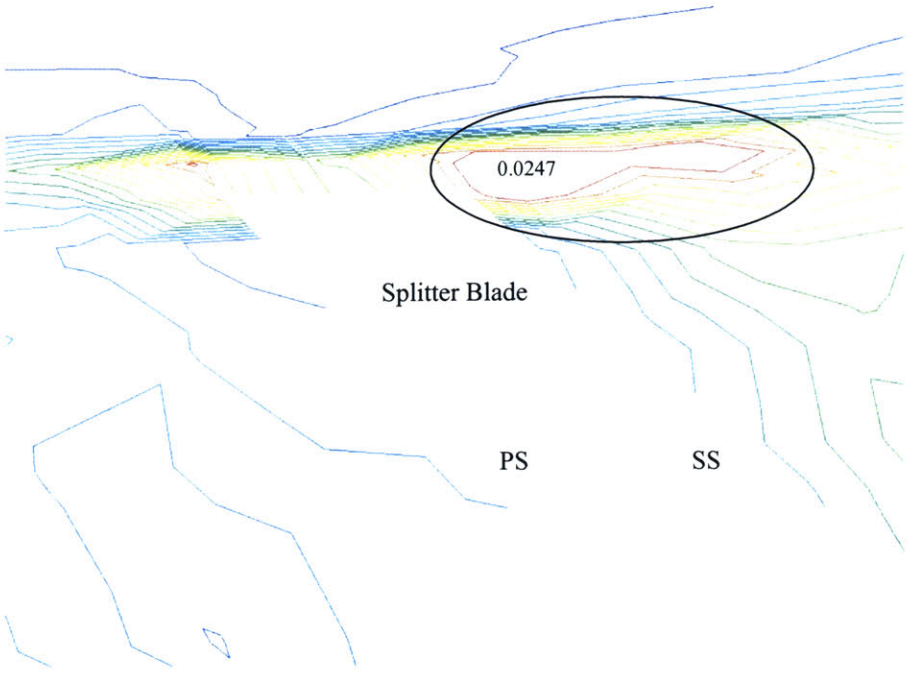

Figure 3-9 Contours of local entropy production rate at splitter normalized by $Tt_1/(\rho_1 V_\Delta t_{BP})$ for vaned diffuser and 6% tip clearance with the value of maximum contour at blade tip indicated -Time step 4.

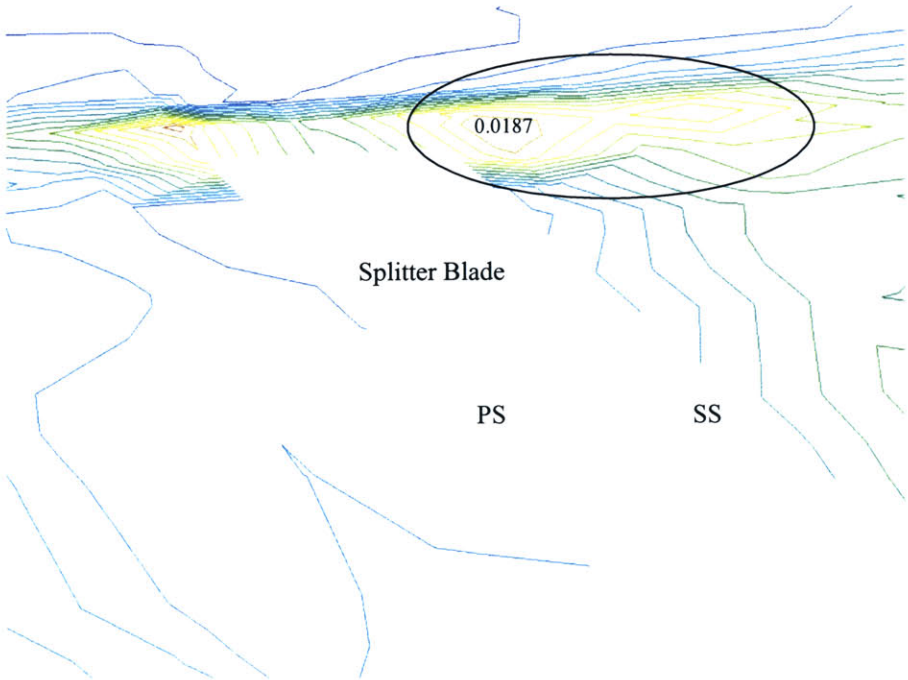

Figure 3-10 Contours of local entropy production rate at splitter normalized by $Tt_1/(\rho_1 V_\Delta t_{BP})$ for vaned diffuser and 6% tip clearance with the value of maximum contour at blade tip indicated -Time step 5.

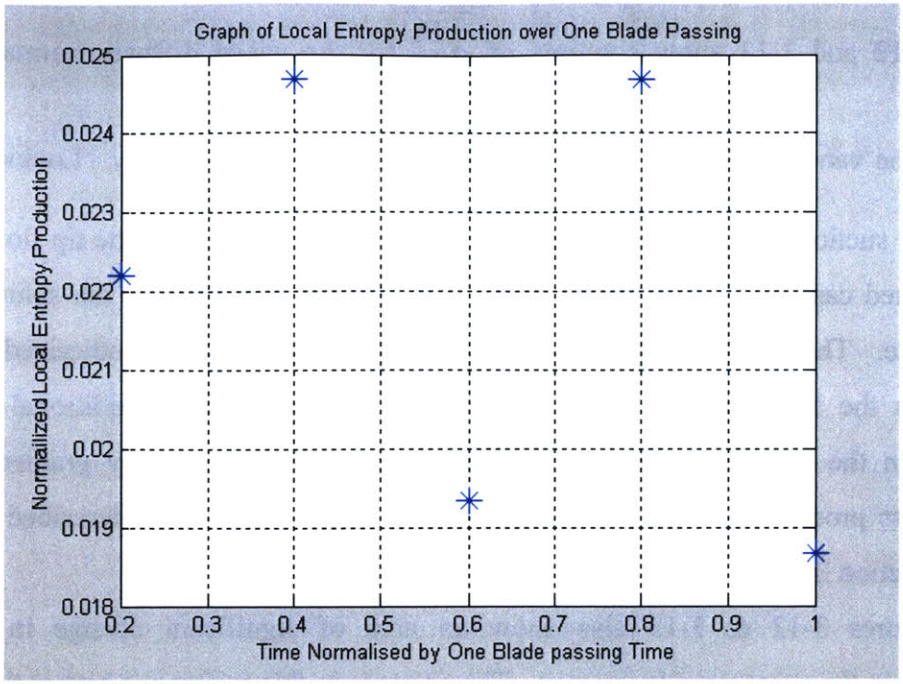

Figure 3-11 Variation of normalized local entropy production with time over one blade passing showing a fluctuation with two peaks.

It is next necessary to identify the source of the unsteadiness and the argument being presented here is that the source of the fluctuation is from the downstream vaned diffuser. Such unsteadiness should have a frequency of two over one-blade passing if it is to be attributed to the downstream vaned diffuser. The reasoning behind this is that for every main blade in the impeller there are two diffuser vanes downstream and thus two peaks. These figures show two peaks at the suction side of the splitter at time steps 2 and 4.

As Shum mentions, it is not important just to identify a fluctuation in entropy production (Indeed it would be intuitively obvious to many readers) due to the downstream vanes. In fact a more important development would be the effect of the downstream vanes on the time averaged value of $\rho\frac{Ds}{Dt}$ compared to the same value in the vaneless diffuser.

Figures 3-12 and 3-13 show contours of $\overline{\rho \frac{Ds}{Dt}}$ for the vaned diffuser normalized by $\overline{\rho \frac{Ds}{Dt}}$ for the vaneless diffuser at 6% and 4% tip clearance respectively. Looking at the main blade suction side, there is an increase in entropy production in the tip flow region for the vaned case over the vaneless case. The same is also true for the splitter blade suction side. These regions are indicated on the figures. Shum hypothesized that the increase in the local rate of entropy production is generated by additional velocity gradients in the tip flow. Shum then linked the additional velocity gradient to the unsteadiness produced by the downstream vanes. This will also be described in more detail in section 3.3.3.

Figures 3-12 & 3-13 also show an area of significant change in entropy production in the pressure side passage. The changes in this region are higher than those in the tip region and were not revealed in Shum's computed flow field for his centrifugal compressor stage. Further investigation into this region shows that streamlines passing through this region originate downstream. This is depicted in figure 3-14 where two streamlines are plotted. One streamline passes through this region and another passes through a similar region in the suction side passage. For these streamlines to travel upstream, they must be in a region of reversed flow. Figure 3-15 shows a plot of the velocity vector normal to a plane where negative value denotes a vector pointing upstream and into the plane. For visualization purposes, red contours are positive vectors and all other colors are negative vectors. The same streamlines are also plotted and show that they are part of this reversed flow region.

This region of high entropy production corresponds to the points where the reversed flow "mixes" with the main-flow and travels downstream. Entropy is produced due to the mixing and similar to the tip flow that is not in the reversed flow region, the unsteadiness downstream introduces an extra velocity gradient that increases entropy production locally.

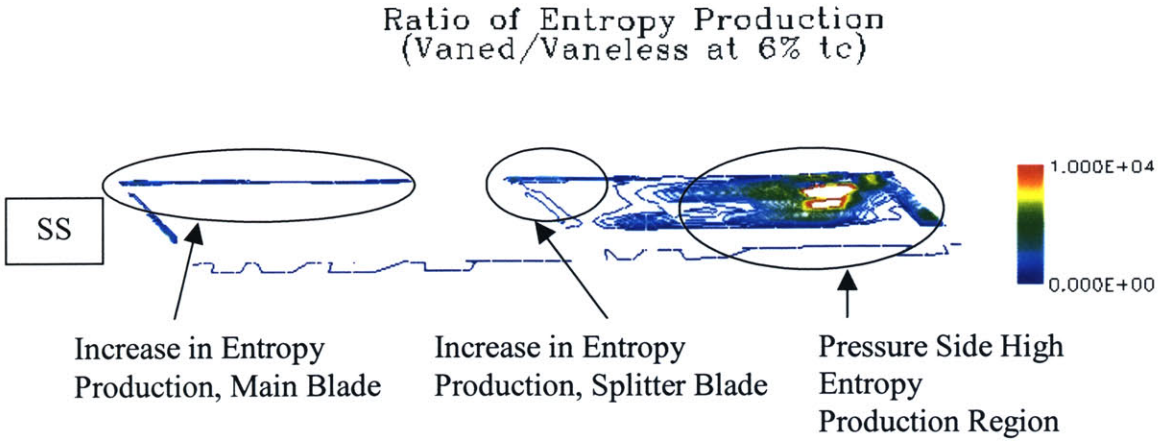

Figure 3-12 Contours of time-averaged volumetric entropy production for the 6% tip clearance, vaned diffuser case normalized by that for the vaneless diffuser case indicating the three regions where entropy production in the vaned diffuser is higher than that in the vaneless diffuser.

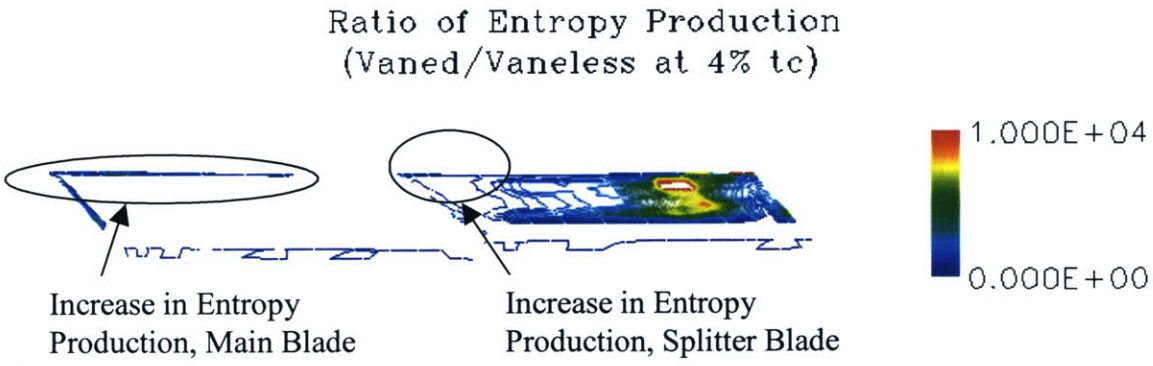

Figure 3-13 Contours of time-averaged volumetric entropy production for the 4% tip clearance, vaned diffuser case normalized by same for the vaneless diffuser case indicating the three regions where entropy production in the vaned diffuser is higher than that in the vaneless diffuser.

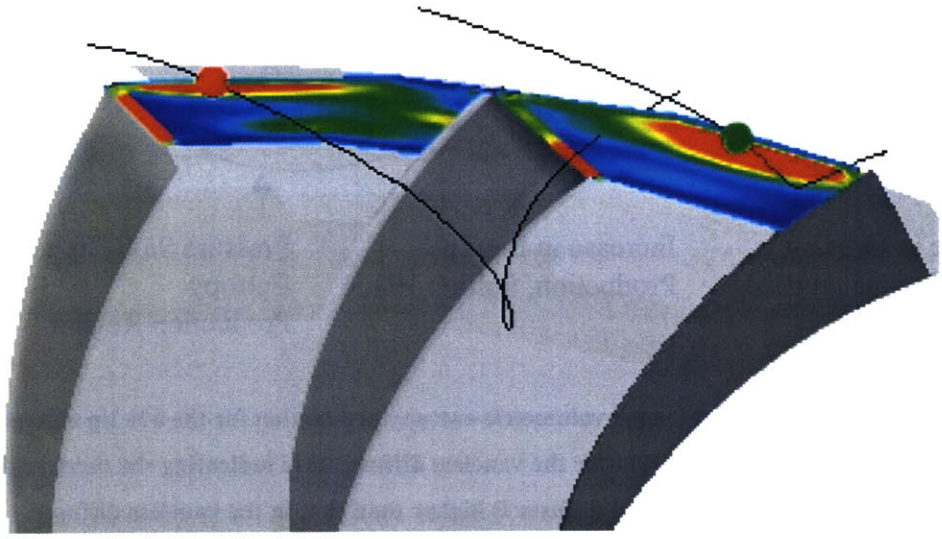

Figure 3-14 Computed pattern of selected streamlines into area of increased entropy production to illustrate that tip flow back leakage exists.

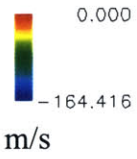

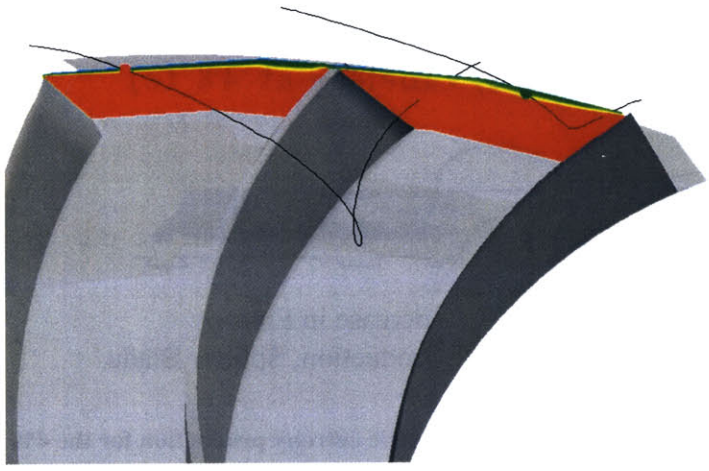

Figure 3-15 Computed distribution of normal velocity vector magnitude and direction at impeller exit plane to depict the region of reversed and forward flow for showing that the tip flow back leakage occurs in the reversed flow.

3.3.3 Origin of Additional Velocity Gradient

Thus far it has been assumed that the downstream unsteadiness produces a fluctuation in the tip flow velocity. Plotting the tip leakage flux over time can explicitly show this. Figures 3-16 to 3-21 plot the non-dimensional tip leakage flux ($\frac{\rho W_{TIP} - \overline{\rho W_{TIP}}}{\overline{\rho U}}$) over one blade passing for radius ratios ($\frac{r}{r_{TE}}$) of 90%, 95% & 99% and tip clearances of 4% and 6%. Figure 3-6 and 3-17 plot the non-dimensional tip leakage flux at the 90% plane for 6% and 4% tip clearance respectively. Figure 3-18 and 3-19 plot the non-dimensional tip leakage flux at the 95% plane for 6% and 4% tip clearance respectively. Figure 3-20 and 3-21 plot the non-dimensional tip leakage flux at the 99% plane for 6% and 4% tip clearance respectively. At 90%, the flux has a large wavelength background fluctuation in both vaned and vaneless cases. Shum [22] advised that this background fluctuation is due to the inherent fluctuation of mass flow in the solution and so is a numerical feature and not a physical property of the flow. In the 95% and 99% cases a mass flux fluctuation over time can be seen with the amplitude increasing with radius ratio. For this to be driven by the downstream unsteadiness, there must be two wavelengths in every blade passing. An inspection of figures 3-20 & 3-21 indicates that this is the case.

Additionally, for the downstream unsteadiness to drive the tip flow fluctuation, the tip loading fluctuation due to the downstream unsteadiness must be in phase with the tip mass flux fluctuation. If the tip mass flux fluctuation is in phase with the tip loading fluctuation then it can be argued that this loading fluctuation drives the mass flux fluctuation. Figure 3-22 compares the tip mass flux over time with the tip loading (ΔP across blade) over time. The two are very close to being in phase and show that the fluctuation in tip flux is certainly driven by the downstream unsteadiness since all conditions for this assumption to be valid are met. The reason for them being slightly out of phase is that they are measured at different points. The loading is measured at the blade tip and the tip leakage mass flux is measured in the tip region.

In summary, this section has shown that the local entropy production in the impeller tip flow increases when a downstream vaned diffuser is introduced. This increase in entropy production was linked to additional velocity gradients.

A region of reversed flow on the casing that allows a streamline to travel upstream, through the splitter blade tip region and mix with the flow in the pressure side passage was exposed. Based on the aforementioned arguments, this flow is affected by the downstream unsteadiness as it passes through the splitter blade tip region. This introduces an additional velocity gradient through the unsteady tip loading that increases the local entropy production. The tip mass flux fluctuation is produced by the loading fluctuation. Therefore there is a direct cause and effect between the tip loading fluctuation due to the downstream unsteadiness and the change in local rate of entropy production.

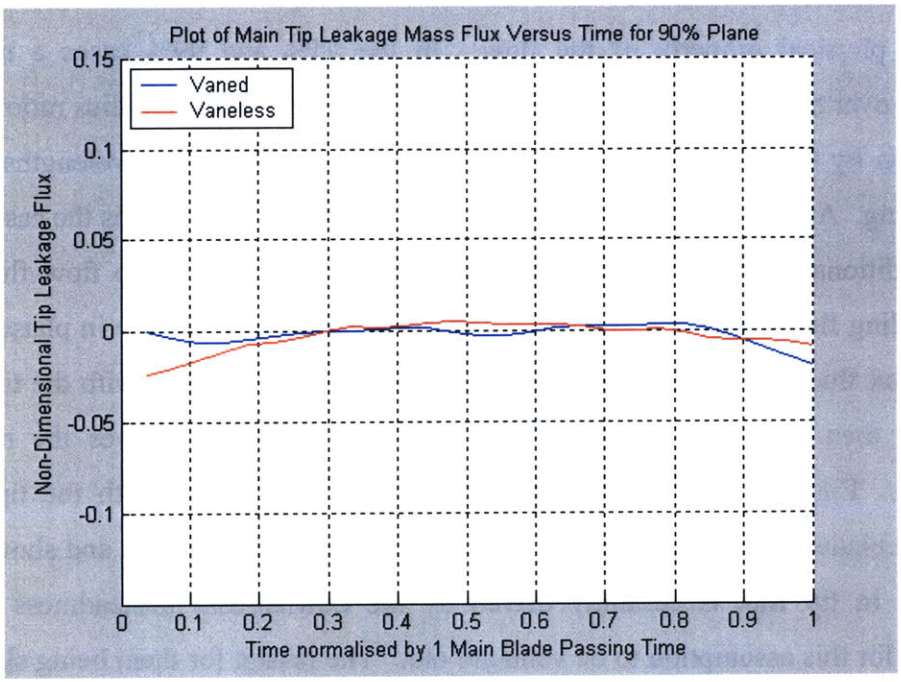

Figure 3-16 Comparison of main blade tip leakage flux over one blade passing at 90% radius ratio and 6% tip clearance for compressor stage with a vaned diffuser against that of one with a vaneless diffuser.

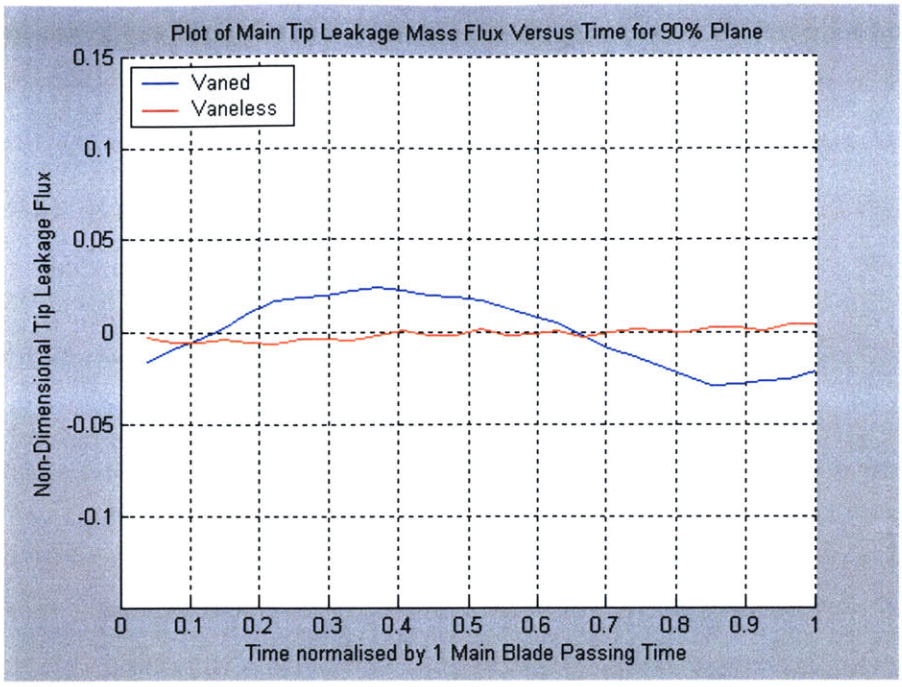

Figure 3-17 Comparison of main blade tip leakage flux over one blade passing at 90% radius ratio and 4% tip clearance for compressor stage with a vaned diffuser against that of one with a vaneless diffuser.

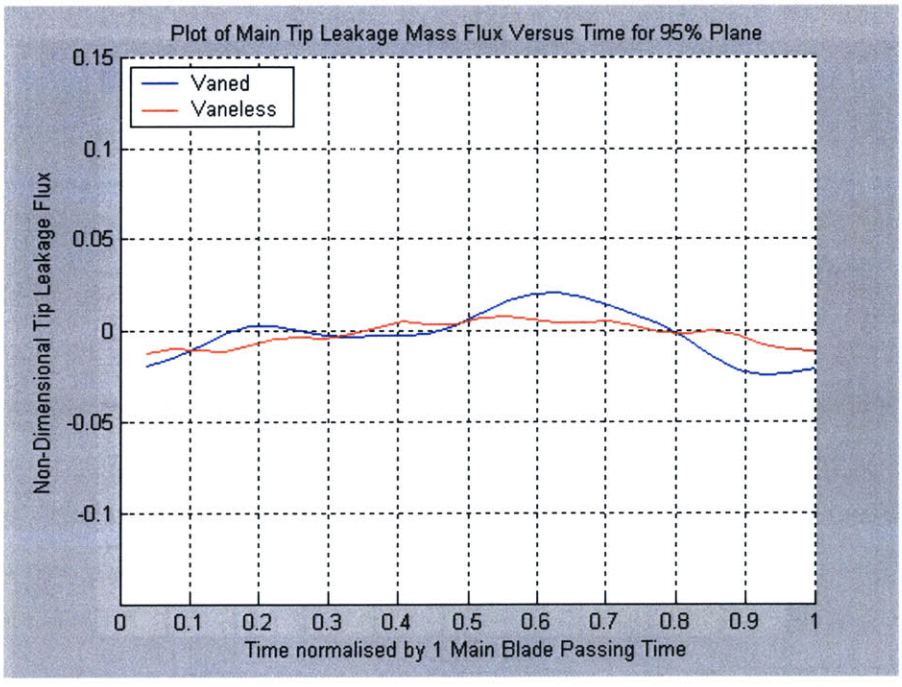

Figure 3-18 Comparison of main blade tip leakage flux over one blade passing at 95% radius ratio and 6% tip clearance for compressor stage with a vaned diffuser against that of one with a vaneless diffuser.

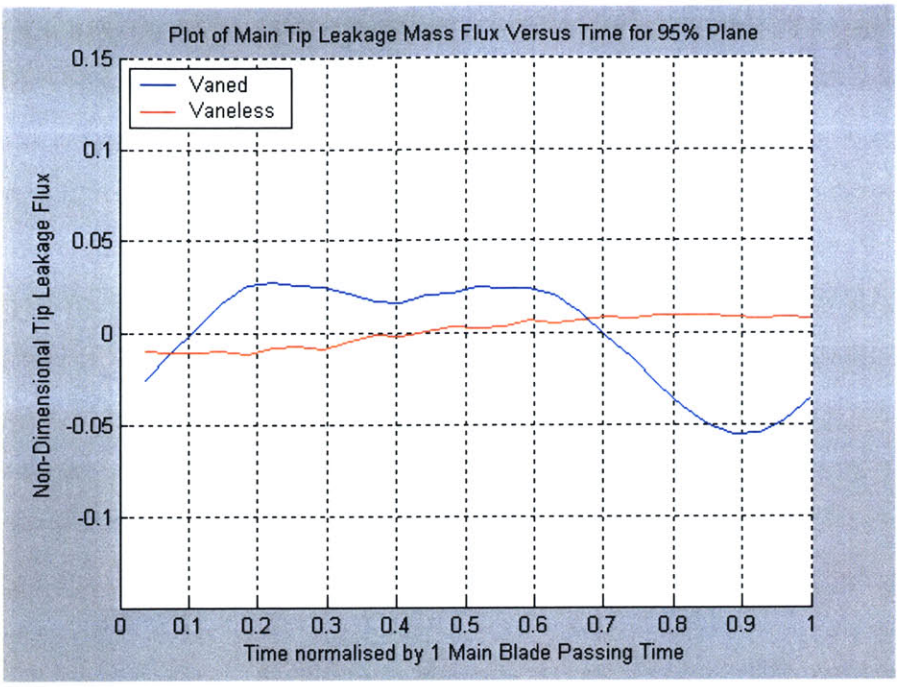

Figure 3-19 Comparison of main blade tip leakage flux over one blade passing at 95% radius ratio and 4% tip clearance for compressor stage with a vaned diffuser against that of one with a vaneless diffuser.

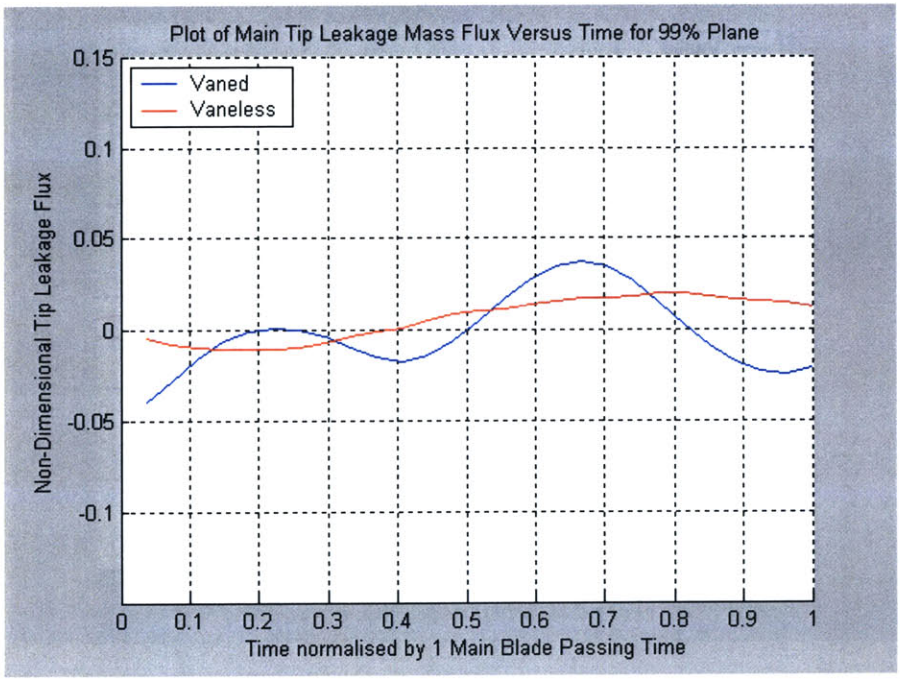

Figure 3-20 Comparison of main blade tip leakage flux over one blade passing at 99% radius ratio and 6% tip clearance for compressor stage with a vaned diffuser against that of one with a vaneless diffuser.

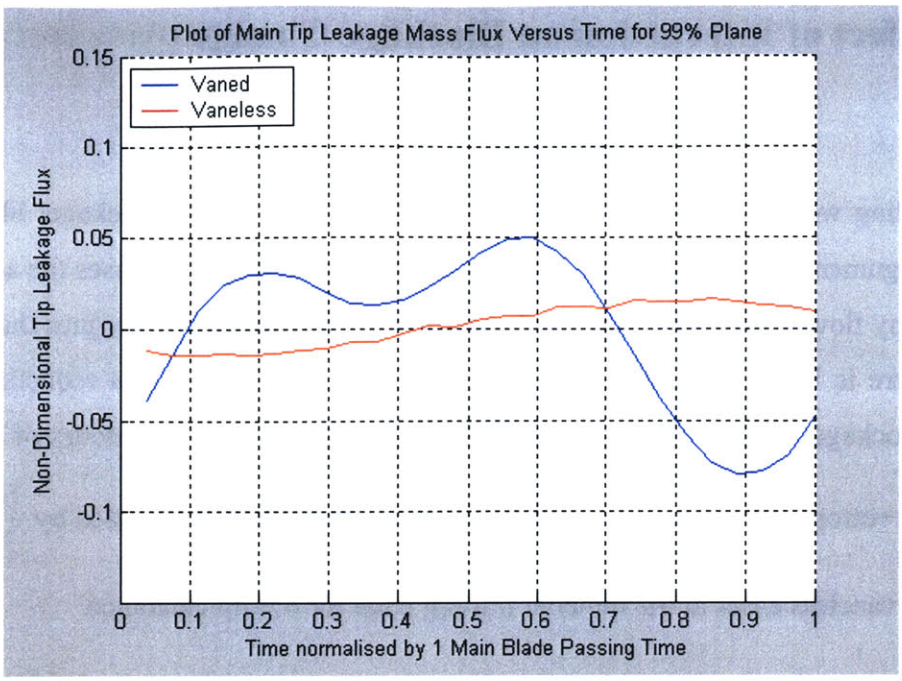

Figure 3-21 Comparison of main blade tip leakage flux over one blade passing at 99% radius ratio and 4% tip clearance for compressor stage with a vaned diffuser against that of one with a vaneless diffuser.

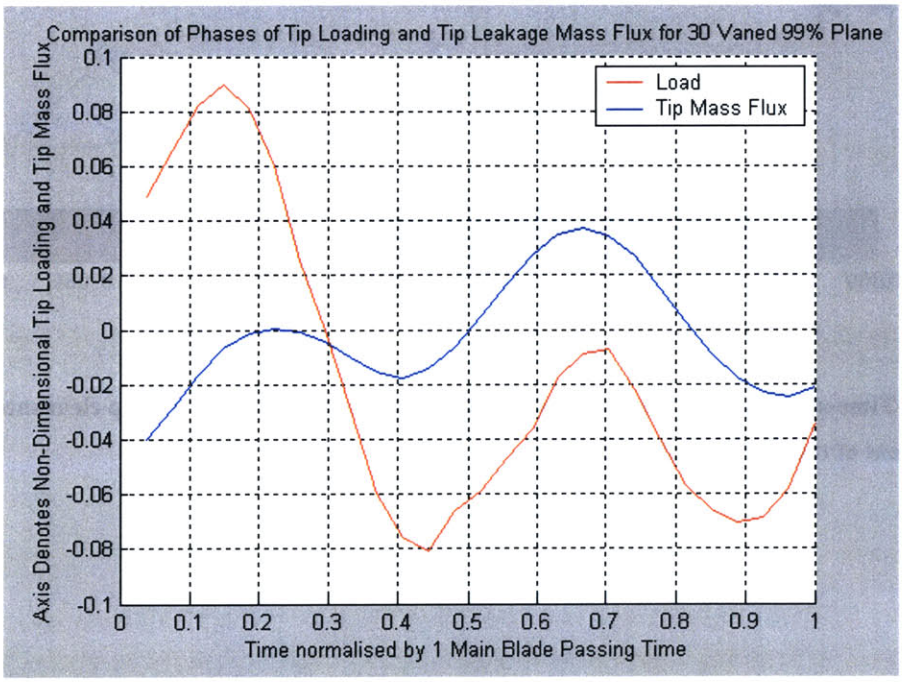

Figure 3-22 Computed results to show that the fluctuations of tip loading and mass flux over one blade passing are in phase for 6% tip clearance case with 30 vaned diffuser.

3.3.4 Effect of Interaction on Blockage Change

When dealing with the effect of the downstream unsteadiness on blockage, Shum [21] uses the argument that an increased impeller-diffuser interaction decreases the amount of high entropy flow leaving from the tip region into the main-flow. He argues that for this reason, there is less high-loss flow in the passage and thus there is a reduction in the passage blockage. Figures 3-23 and 3-24 show the time-averaged contours of s_2-s_1 (the increase in entropy from impeller leading edge to trailing edge) normalized by $\frac{U^2}{Tt_1}$ for the vaned and vaneless cases at the impeller trailing edge for 6% tip clearance.

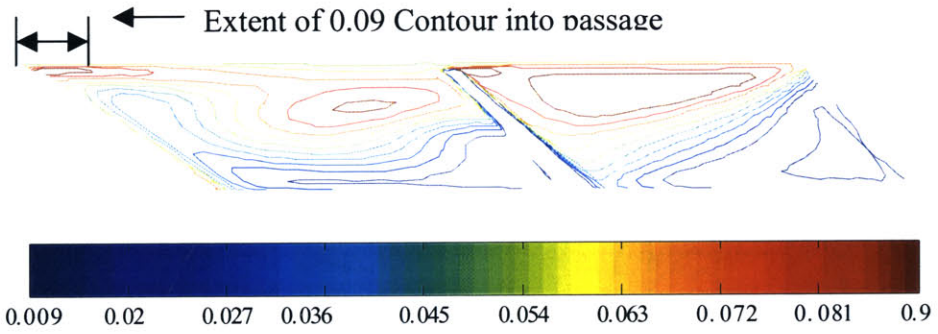

Figure 3-23 Time-averaged contours of (s_2-s_1) for the vaneless diffuser and 6% tip clearance impeller with the extent of the 0.09 contour indicated.

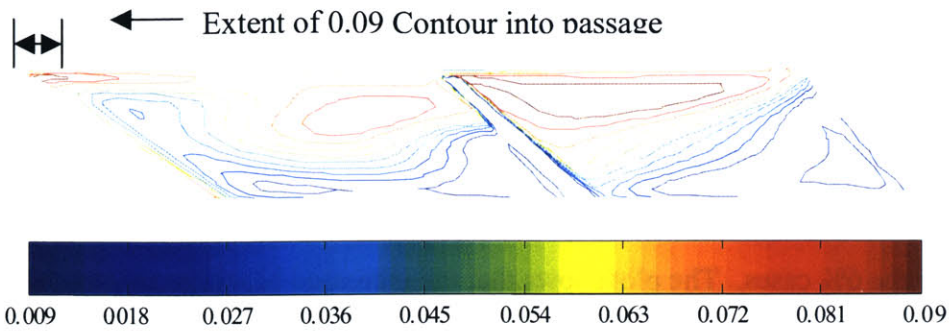

Figure 3-24 Time-averaged contours of (s_2-s_1) for the vaned diffuser and 6% tip clearance impeller with the extent of the 0.09 contour indicated.

Figure 3-23 indicates a region in the trailing edge of the impeller with a vaneless diffuser called the "Extent of 0.09 contour into passage". This 0.09 contour is of interested because it is the contour that depicts the high entropy tip flow. This contour extends approximately 10% of the local pitch into the blade passage. This region is also shown for the vaned diffuser case in figure 3-24. Here however, the extension of the 0.09 contour is approximately 5% of the pitch into the passage. Therefore this contour extends further into the blade passage in the vaneless case and shows that high entropy flow from the tip region, flows further in to the passage in the vaneless diffuser case. This agrees with Shum's findings and is the basis of his argument for observed reduction in blockage.

This author chooses a different explanation. The calculation for blockage used in this thesis differs from that used in similar investigations ([17], [21]). Blockage in this case is defined as the mass averaged product of density and the projection of the relative velocity vector on the through-flow (subscript TF) normal vector. If the blockage were to decrease, the time averaged through-flow mass flux ($\overline{\rho W_{TF}}$) would also decrease because of continuity and the fact that decreased blockage implies increased effective area. For blockage to decrease, the mass flux of the blocked region must increase. In this investigation, the blockage will be shown in section 3.4.2 to decrease in the 6% tip clearance case when a vaned diffuser is introduced. Therefore, in a plot of

$\overline{(\rho W_{TF})}_{vaned} - \overline{(\rho W_{TF})}_{vaneless}$, the contours in the main-flow will be negative because the flow area has increased in the vaned case while those in the defect regions will be positive because the magnitude of this defect has been reduced. This logic can be used to locate the regions that blockage has increased due to the downstream vanes. Figure 3.25 shows the contours of $\overline{(\rho W_{TF})}_{vaned} - \overline{(\rho W_{TF})}_{vaneless}$ at the trailing edge of the impeller blade for the 6% cases. The plot shows that the increased blockage region coincides with the region of high rate of entropy production. In other words, the tip flow region that has increased entropy production also has decreased blockage when the vaned diffuser is added. This leads us to the conclusion that not only does the downstream unsteadiness increase the entropy production in the tip flow; it also reduces the time averaged blockage.

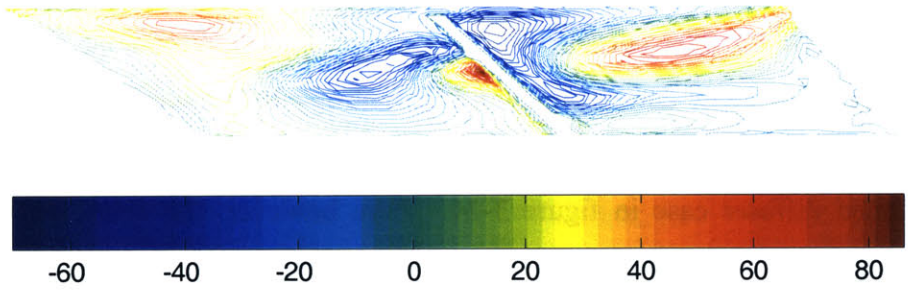

Figure 3-25 Contours of $\overline{(\rho W_{TF})}_{vaned} - \overline{(\rho W_{TF})}_{vaneless}$ for 6% tip clearance.

In summary, this section has identified that a reduction in blockage occurs in the tip flow when a vaned diffuser is introduced downstream of an impeller. This reduction in blockage can be linked to the downstream unsteadiness by the same logic used when demonstrating the increase in entropy production in section 3.3.2. Therefore, one effect of the interaction is a reduction in tip flow blockage.

3.3.5 Effect of Interaction on Slip Change

Shum argues that the change in slip encountered in his investigation is predominantly due to the pressure field produced by the vanes. He shows that the region of reversed flow encountered at the casing is too small to have a significant effect on the overall slip. In this investigation, the region of reversed flow is slightly bigger but the mass flux of this region is significantly smaller than the main flow mass flux and therefore the tangential velocities in the reversed region will have little effect on the overall mass averaged tangential velocity of radial planes. Therefore, the same argument as Shum can be used and the change in slip can be attributed to inviscid effects of the downstream diffuser.

The slip angle decreases by .01 radians (0.6°) for the 6% tip clearance case when the downstream vanes are introduced. This slip is important when looking at the downstream vaned diffuser performance because Philips [18] found that the stator performance depends on the direction of the main-flow velocity vector, which is directly influenced by the slip angle. This will be examined in section 3.5 below.

3.4 Analysis of Influence Coefficient Trends

3.4.1 Introduction

The preceding section described and explained how the unsteady interaction between the downstream diffuser and upstream impeller changed the performance of the impeller. This section presents the changes so computed.

Shum's one-dimensional flow model shows that the three parameters needed for an adequate delineation of resulting change in performance are change in entropy production, change in flow blockage and change in slip angle (Δs, ΔB & $\Delta\theta$). Their effects are described in the one-dimensional model using the entropy, blockage and slip influence coefficients, C_S, C_A & C_θ respectively. Analyzing these and their effects on the performance of the impeller can shed light on how the change in performance from vaneless to vaned diffuser stage occurred.

3.4.2 Description of Blockage Influence Coefficient's Effect on Total Pressure

In this study, the effect of the downstream vanes on the blockage in the impeller is important and will be studied using the blockage coefficient C_A introduced in *2.4.2.3*. It is important to point out that this coefficient measures the change in performance of an impeller due to a change in the blockage. This coefficient was developed in [21] and its definition can be seen in this text in section *2.4.2.3*.

In this study, the only geometric difference between compared cases will be in the diffuser. In each comparison, the configurations are identical except one diffuser will be vaned and the other vaneless. Thus, the only source of blockage change will be due to the impeller-diffuser interaction. Also, in the comparisons, the vaneless case is seen as

the base (benchmark) and the vaned case is compared to this. Therefore, the blockage coefficient measures the contribution of the downstream unsteadiness to the impeller performance through its influence on the impeller blockage generation. Figure 3-26 shows the change in non-dimensional total pressure (based on $\frac{1}{2}\rho U^2$) in the impeller due to a change in blockage generated by adding a vaned diffuser to the stage as calculated by Shum's one-dimensional flow model.

It is interesting to note that at 0% tip clearance the effect of blockage is to reduce the non-dimensional total pressure in the stage. Figure 3-2 in section 3.2 showed that the change in non-dimensional total pressure was negligible at 0% tip clearance. This indicates that the decrease in performance due to blockage in figure 3-26 at 0% tip clearance was balanced by an increase in performance due to some other flow process. Sections 3.4.3 and 3.4.4 will describe the entropy and slip coefficients in detail but at this point it is appropriate to refer to the results. Both these two coefficients show an increase in the total pressure ratio at 0% tip clearance and balance the negative impact on performance due to blockage change.

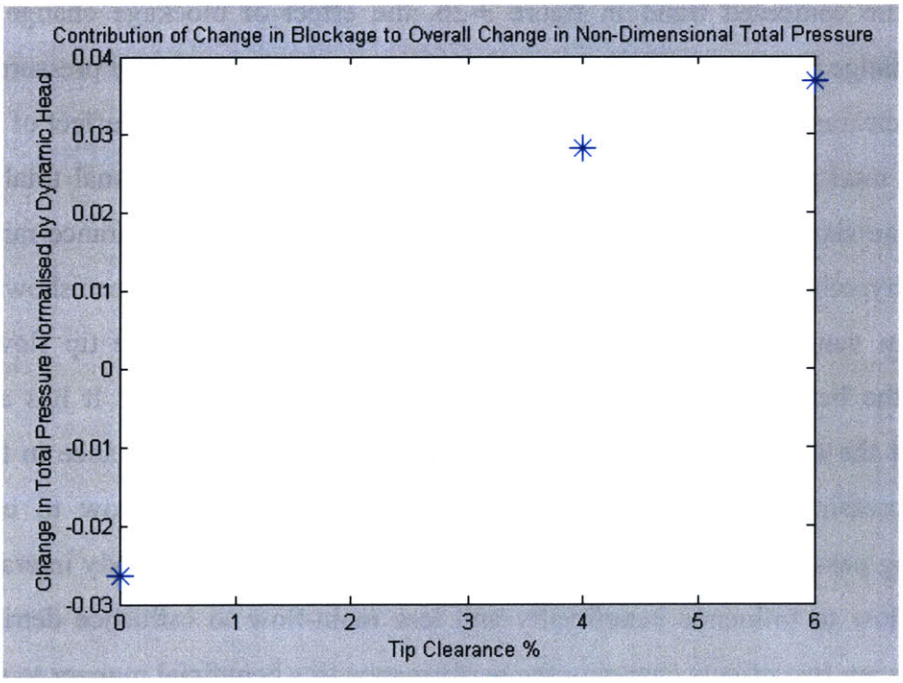

Figure 3-26 Effect of blockage change on change in non-dimensional total pressure with tip clearance as calculated by the one-dimensional flow model.

To understand why the vaned diffuser changes the total pressure ratio through blockage generation at 0% tip clearance a few details must first be explained. Shum [21] found that increasing blockage reduces the total pressure in the stage and decreasing blockage does the opposite. While it may seem obvious, it should be pointed out that at 0% tip clearance there will also be 0 tip flow for the impeller-diffuser interaction to influence. This means that any change in blockage is produced in the mean-flow. Therefore, the reduction in total pressure seen in this plot means that the blockage in the passage (mean-flow) has increased due to the addition of the vaned diffuser. Shum [21] and Graf [11] also concluded from their research that downstream unsteadiness increased the time-averaged blockage in the mainflow. The conclusion that the mainflow has increased blockage will be used in the arguments that follow.

In figure 3-26, as tip clearance increases the contribution of blockage to the performance starts to increase. There is a point where the overall contribution of blockage crosses the abscissa. Therefore, above a certain tip clearance, the influence of the impeller-diffuser interaction with regard to blockage in the tip flow is beneficial enough that it outweighs its detrimental effect in the mainflow.

From the computed trend in figure 3-26, the effect of blockage change on total pressure change increases by approximately 0.06 (non-dimensional total pressure change) over a tip clearance range of 0%-4%. From 4%-6% tip clearance the effect of blockage change on total pressure change is approximately 0.01 (non-dimensional total pressure change), one sixth of the change in the first two thirds of the tip clearance range. The following hypothesis can be used to explain this trend: It has already been shown that the downstream vaned diffuser decreases the blockage produced by the tip flow and so enhances the beneficial effect of blockage change in performance. It has also been shown that the downstream vane has a detrimental effect on performance in the main-flow. Increasing the tip clearance allows a larger volume tip flow to cross into neighboring passages. As the volume of tip flow increases, the unsteady interaction has more tip-flow to influence beneficially and less main-flow to influence detrimentally. Thus, there are two effects changing the performance in a beneficial manner to produce a larger computed change in non-dimensional total pressure with tip-clearance in the 0% to 4% range. Eventually, as tip clearance increases and tip flow dominates the passage, any

change in blockage in the main-flow region will become negligible. At this stage only the tip clearance blockage reduction increases the performance. This accounts for the smaller observed change in non-dimensional total pressure with tip clearance above 4% tip clearance.

3.4.3 Description of Entropy Influence Coefficient's Effect on Total Pressure

The second influence coefficient is the entropy influence coefficient and this measures the change in performance of an impeller due to a change in the entropy generation. Figure 3-27 shows the effect of the entropy influence coefficient on the total pressure rise. The trend with tip clearance is non monotonic with a local maximum. The impact of the entropy influence coefficient as reflected in the one-dimensional model described in section 2.4.2.3 shows the importance of viscous dissipation to impeller total pressure ratio and efficiency.

The trend in figure 3-27 implies that the downstream 30-vaned diffuser has a beneficial effect on the 0% tip clearance impeller by decreasing entropy production (hence a positive value for the entropy influence coefficient). As tip clearance increases, the beneficial effect of the entropy influence coefficient on the change in non-dimensional total pressure increases until a turn around point. At this turn around point, the trend starts to reverse and the beneficial effect on non-dimensional total pressure decreases. Thus there exists a situation where the beneficial effect of the downstream vaned diffuser with regard to entropy generation and hence change in non-dimensional total pressure is optimized.

Shum's results show that the contribution of entropy influence coefficient to the change in impeller performance is highest when the overall change in performance due to the downstream diffuser is at its maximum (at medium interaction point). This is in accord with the results in this thesis.

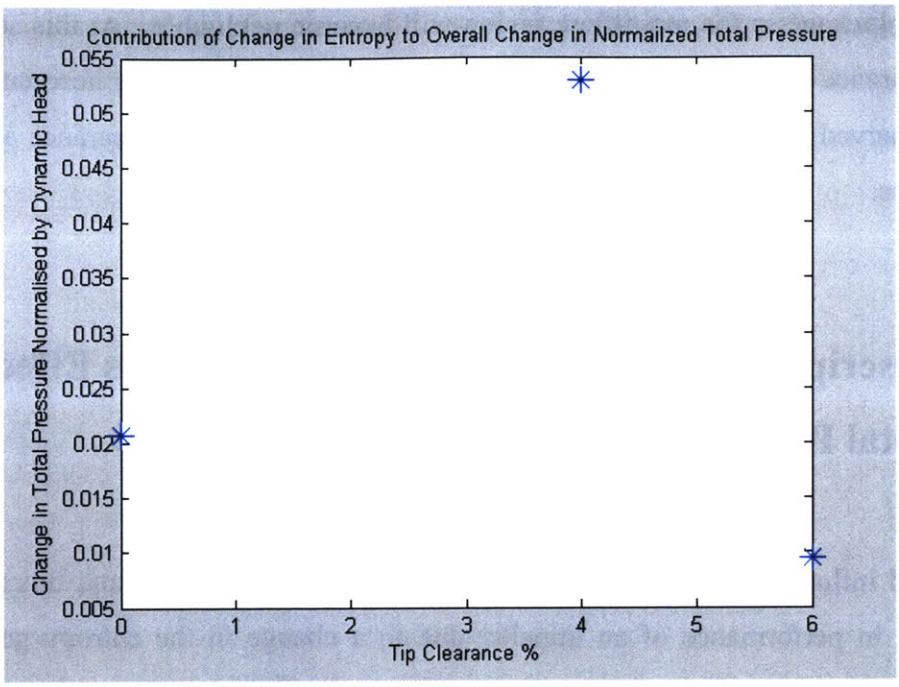

Figure 3-27 Effect of entropy change on change in non-dimensional total pressure versus tip clearance as calculated by the one-dimensional flow model [21]; computed trend is non-monotonical.

3.4.4 Description of Slip Influence Coefficient's Effect on Total Pressure

Slip coefficient, as can be seen from figure 3-28, has the least effect on the impeller performance in this study. It only becomes significant at large impeller tip clearances. It will be seen in section 3.5 that the flow alignment with the diffuser vanes and hence slip angle has a noticeable impact on the performance of the vaned diffuser.

The change in the slip angle is due to inviscid effect of the downstream pressure field associated with the presence of a downstream vaned diffuser. The contribution of the slip coefficient to non-dimensional total pressure change is generally beneficial except at a region around the 4% tip clearance.

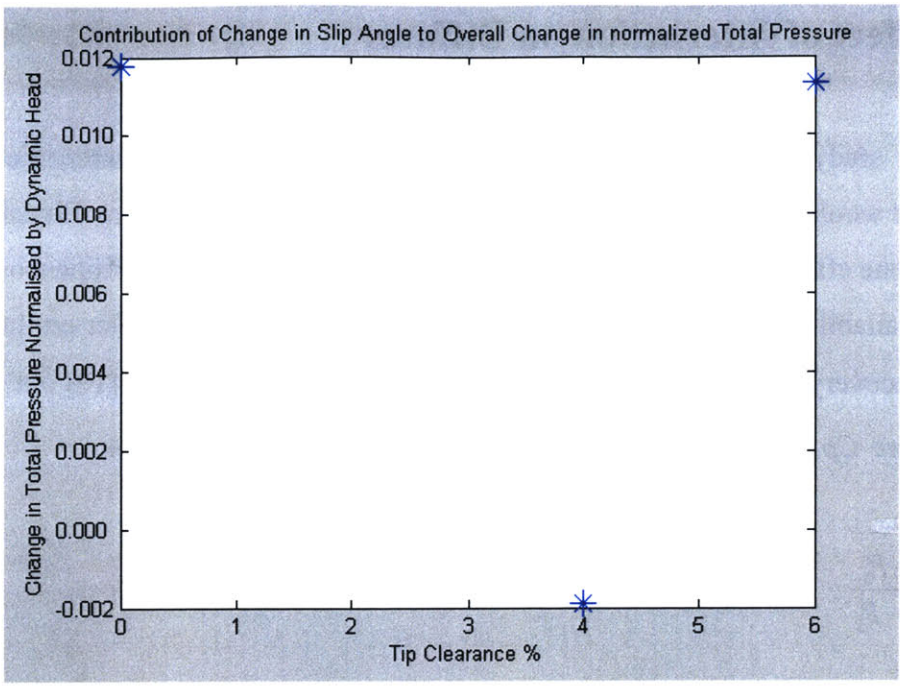

Figure 3-28 Effect of change in slip angle on change in non-dimensional total pressure with tip clearance as calculated by the one-dimensional flow model [21]; computed trend is non-monotonical.

3.5 Effect of Interaction on Diffuser

While this study mainly deals with effect of the impeller-diffuser interaction on the impeller, it would also be of interest to show the effect on the diffuser. Elucidating the diffuser alone effect on the stage performance would accomplish this. Filipenco *et al.* [10] used an availability average to neglect the effect of the upstream impeller on the diffuser pressure recovery, Cp. The definitions of Cp and Cp_{Ψ} are derived in [10] but are given below where Cp_{Ψ} is the availability averaged diffuser pressure recovery.

$$Cp = \frac{P_4 - P_3}{Pt_3 - P_3}$$

$$Cp_{\Psi} = \frac{P_4 - P_3}{Pt_{\Psi 3} - p_3}$$

$$\text{where} \quad Pt_{\Psi} = \exp\left[\frac{\int \ln(Pt)\, d\dot{m}}{\int d\dot{m}}\right]$$

Table 3-2 shows the performance of the diffuser in all six cases based on mass averaged and availability-averaged descriptions. It can be seen from the table that the difference between the mass averaged and availability averaged Cp is quite small. This is in agreement with Filipenco *et al.* [10] who found that the discrepancy between mass averaged and availability-averaged total pressure was never greater than 1.6% of either pressure recovery value. In this study the discrepancy was always less than 1% of either pressure recovery value.

The results also show that increasing the tip clearance results in an increase in the discrepancy between availability and mass averages. This however will not be a

significant factor in the performance of the machine as the trends asymptotically reach a value that is approximated as lower than 1%. The results indicate that either averaging technique can be used to describe the performance of the diffuser in this study.

Case	Cp (mass-averaged)	Cp (availability)	% Discrepancy
Vaneless			
0% TC	0.347	0.347	0.173
4% TC	0.336	0.338	0.566
6% TC	0.363	0.365	0.579
Vaned			
0% TC	0.637	0.638	0.236
4% TC	0.534	0.537	0.637
6% TC	0.345	0.348	0.696

Table 3-2 Performance of vaned and vaneless diffusers in tip clearance variation study using both mass-averaged and availability averaged data.

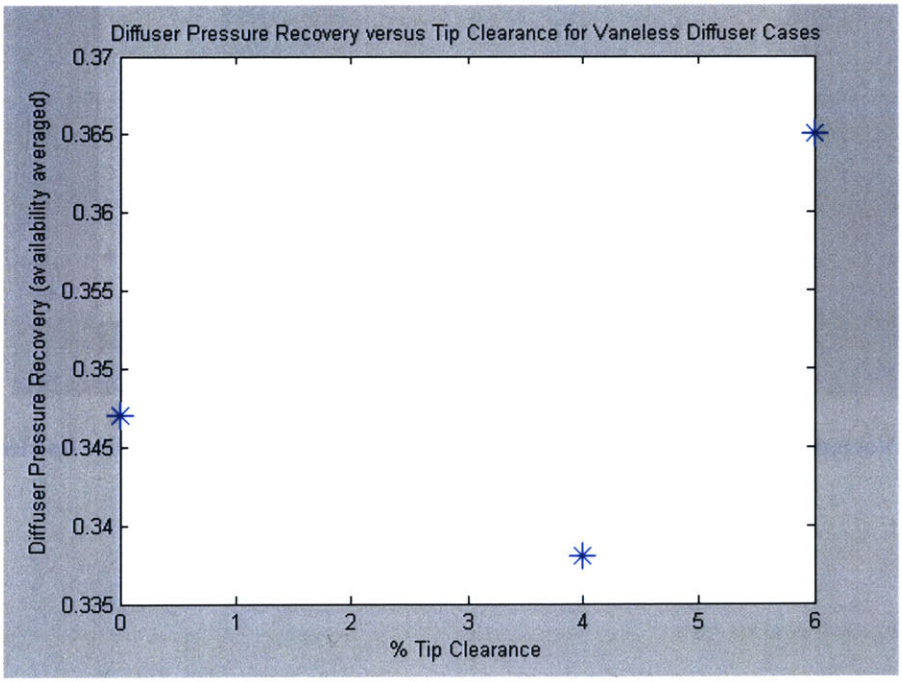

Figure 3-29 Variation of diffuser pressure recovery in vaneless diffusers with impeller tip clearance; the computed trend is non-monotonic.

The computed pressure recovery, Cp, for the vaneless diffuser shows a non-monotonical variation: a local minimum for the configuration with 4% tip clearance can be inferred from figure 3-29. The variation is not as large as that for the vaned diffuser situation but shows the need for isolating the effect of tip clearance on diffuser performance. A numbers of authors [10,18,21] linked the change in vaned diffuser performance to the absolute velocity angle of the flow at inlet or more importantly the alignment of the inlet flow with the diffuser vanes. Figure 3-30 shows that the dominant effect on the change in diffuser performance is diffuser inlet flow angle. This is in agreement with findings from other authors [10,18,21].

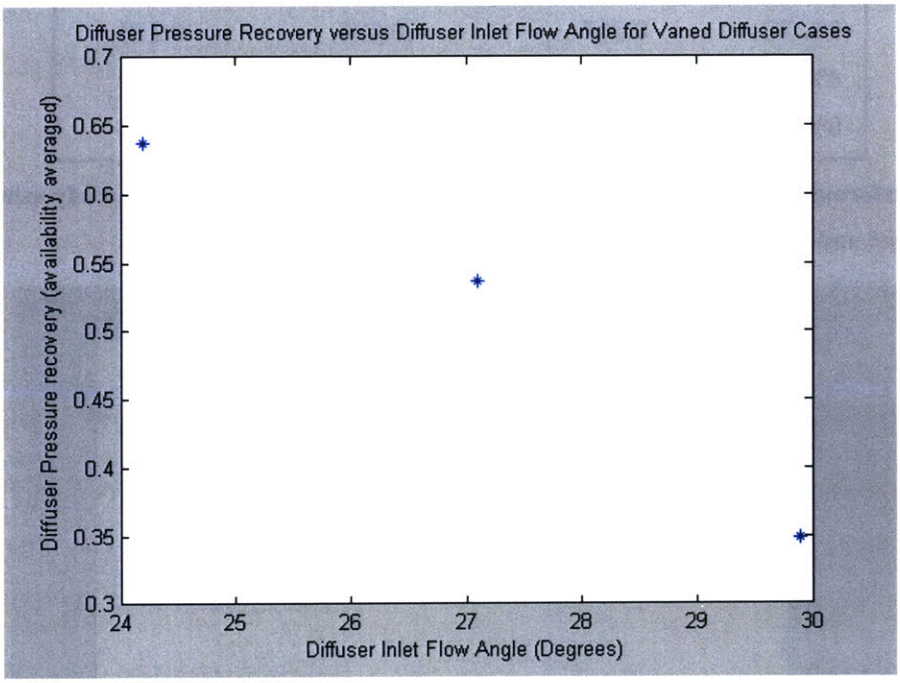

Figure 3-30 Variation of diffuser pressure recovery in vaned diffusers with impeller tip clearance.

3.6 Summary

This chapter demonstrated the role that the impeller tip flow plays on the impeller-diffuser interaction and its impact on performance. For stages with vaned or vaneless diffusers, the efficiency and total pressure ratios decrease with tip clearance. The noticeable difference between the trends for vaned and vaneless diffuser stages is that a vaneless diffuser stage produces performance trends that are linearly dependent ([1], [5]) on tip clearance, this is not true for vaned diffuser stages.

The total pressure ratio of an impeller with vaned diffuser at a given tip clearance is higher than that with a vaneless diffuser over the range of data points investigated in this study. The difference between the two appears to indicate the existence of a local maximum. The trends for efficiency follow a similar trend to that of total pressure ratio with a local maximum.

The downstream unsteadiness associated with the vaned diffuser was shown to drive an unsteady pressure loading on the impeller blade tip. This unsteady loading produced an additional velocity gradient in the tip flow. This additional velocity gradient acts to reduce the blockage associated with the tip flow below that in the impeller-vaneless diffuser stage. However the unsteady interaction also acts to increase the blockage in the core/main flow above that in the impeller-vaneless diffuser stage (where unsteady interaction is absent). The former effect becomes dominant over the latter effect on blockage change as the impeller tip clearance is increased. In addition to affecting a change in blockage, this additional velocity gradient also acts to increase the viscous dissipation in the tip flow.

The diffuser performance was shown to be dependent mostly on the flow alignment with the diffuser vanes. This was in agreement with Philips [18] who showed that vaned diffuser performance was far more sensitive to flow alignment than axial distortions.

Chapter 4

Effects of Diffuser Vane Counts on Centrifugal Compressor Performance

4.1 Introduction

This chapter addresses the second research issue delineated in chapter 1 and investigates the effect of diffuser blade count on the performance of the upstream impeller. This is a question of engineering interest. Cumpsty [5] states that in his opinion it is not a well-understood topic and that it has an important influence on stage performance. He quotes results from other authors [4, 13] who show that the stage performance is dependent upon the diffuser vane number.

Vaned diffusers imply unsteadiness in the impeller frame and hence have an upstream influence on the impeller. This thesis and others ([21]) have demonstrated that this upstream influence can have both a beneficial and detrimental effect on the performance of the impeller. Parametric studies including that in chapter three of this thesis and [21] have been performed to isolate the diffuser's effect on the impeller by varying tip clearance and the radial distance between the impeller and the diffuser. The next step is to isolate how changing the blade count in the diffuser will affect the impeller performance. This chapter describes the findings of such a study.

The impeller efficiency of three different stage configurations are compared to show how the performance of the impeller changes with blade count. The geometrical differences in the three configurations are in the diffuser. One configuration consists of a

vaneless diffuser while the other two configurations are vaned with blade counts of 15 and 30. The results of this investigation show that there is a blade count that optimizes the performance of the impeller. This is compared with results that Shum [21] found for the dependence of impeller efficiency on impeller-diffuser gap size. The results indicate that the two phenomena are somewhat analogous.

4.2 A Hypothesis for Upstream Influence of Diffuser

Shum [21] showed how changing the radial distance between the impeller and the diffuser affects the performance of the impeller. He identified an optimal radial gap between the impeller and diffuser and linked the performance of the impeller to the unsteady response of the tip flow to the diffuser pressure field.

The upstream influence of the diffuser has a length scale equal to the pitch of the diffuser at leading edge. Decreasing the number of blades increases the pitch and hence the upstream influence of the diffuser unsteadiness.

Equation 4.1 describes the upstream decay of a periodic, circumferentially non-uniform pressure disturbance (Greitzer *et al.* [12]).

$$p'(x,y) = \left|p'(0,y)\right| e^{2\pi x / L} \tag{4.1}$$

In this equation the upstream influence of the lowest harmonic is being shown with x being the distance from the disturbance origin and L the length scale of the disturbance. In an impeller-diffuser interaction, x at the impeller trailing edge is the radial gap between the impeller and diffuser, G while L is the pitch of the diffuser leading edge, S. Thus equation 4.1 can be re-written as;

$$p'(x,y) = \left|p'(0,y)\right| e^{2\pi G / S} \tag{4.2}$$

Both G and S have length scales and so the ratio of G/S is non-dimensional. It can be deduced from equation 4.2 that if the G/S ratio (gap-to-pitch ratio) is held constant then the upstream influence of the pressure disturbance on the impeller trailing edge can be kept constant. An implication of engineering interest is given below.

The blade count, N, is inversely proportional to the pitch of the diffuser S. If the blade count doubles then the pitch will half and the gap-to-pitch ratio will double, if however G doubles the gap-to-pitch ratio will also double. Therefore, changing the

diffuser blade count and the impeller/diffuser gap size has the same effect on the gap-to-pitch ratio and hence the upstream influence of the diffuser. It is hypothesized here that altering the diffuser blade count is analogous to changing the gap size.

4.3 Results

The three cases that were performed as part of this study allow for an assessment of the hypothesis presented in section 4.2. Table 4-1 shows the performance of the impeller for 3 different diffuser vane counts. The computed results given in table 4-1 indicate that both the efficiency and the total pressure ratio do not scale monotonically with blade count or gap-to-pitch ratio.

Figure 4-1 shows the total pressure ratio across the impeller computed here for three different gap-to-pitch ratio obtained by changing diffuser vane count while figure 4-2 shows the total pressure ratio across the impeller for three different gap-to-pitch ratio obtained by changing the impeller-diffuser gap [21]. The results in both these figures imply that a situation exists in which the performance is optimal. More importantly, one can deduce from the similarity between the trends that the optimum impeller performance appears to be characterized by the gap-to-pitch ratio. The results however are not extensive enough to prove this hypothesis and additional work is needed.

Case	Vane Count	Tip Clearance	Total Pressure Ratio	Efficiency	Gap-to-Pitch Ratio
3	0	6%	3.872	87.5%	1
6	30	6%	3.919	87.7%	0.407
7	15	6%	3.910	86.4%	0.204

Table 4-1 Computed impeller performance for impeller-diffuser stage with various vane counts.

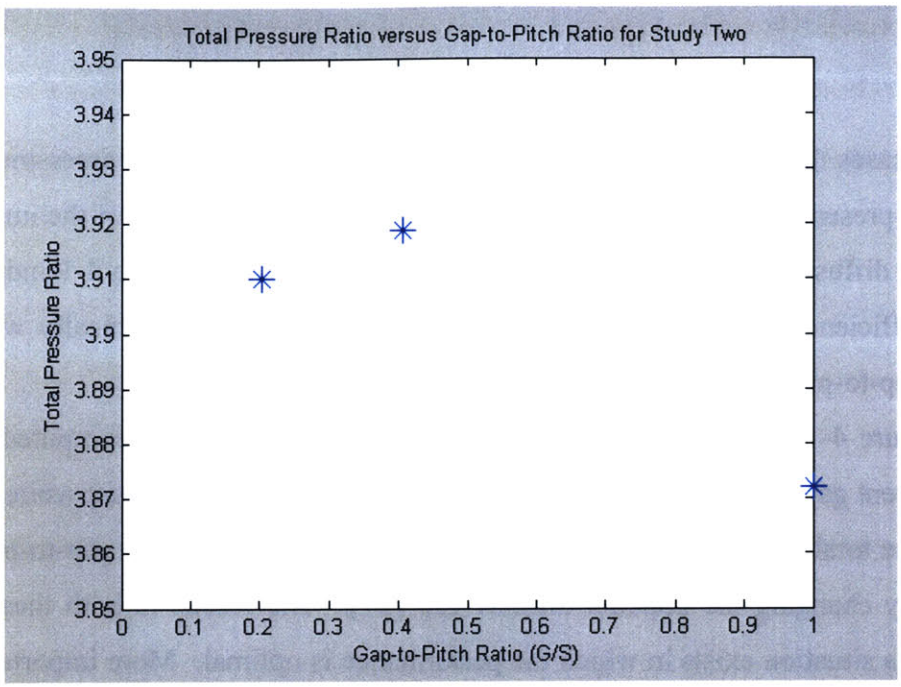

Figure 4-1 Change in impeller total pressure ratio with gap-to-pitch ratio varied through diffuser vane count; the computed trend is non-monotonic.

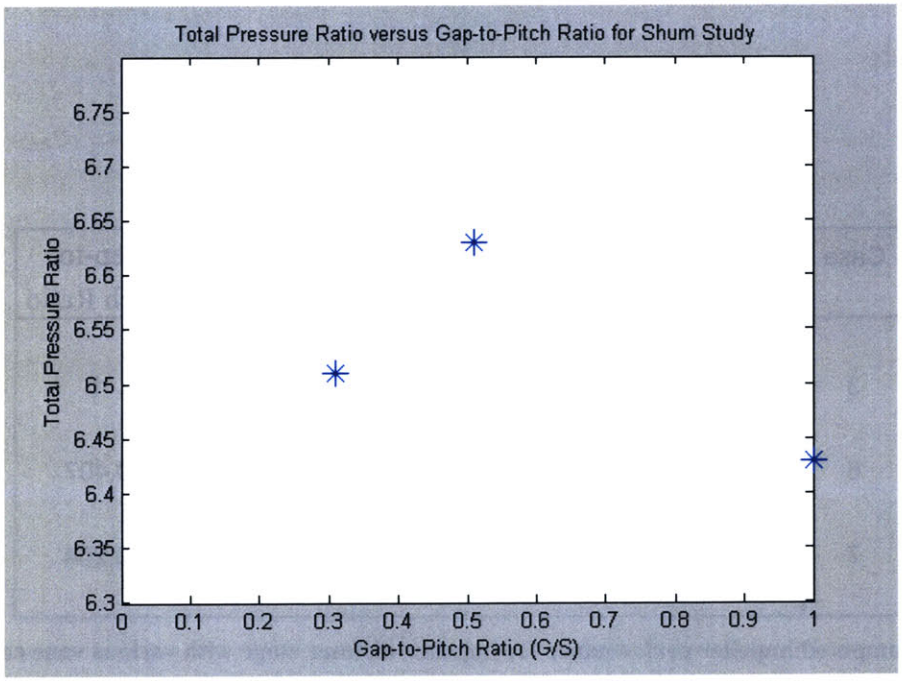

Figure 4-2 Change in impeller total pressure ratio with gap-to-pitch ratio varied through impeller-diffuser gap [21] for contrasting with the results in figure 4-1.

Figure 4-3 demonstrates the dependence of impeller efficiency on the vane count. This can again be compared to the results in Shum's study presented in figure 4-4. The trends for efficiency are similar to those observed for total pressure ratio shown in figures 4-1 and 4-2.

These results have been obtained for two different centrifugal compressor stages with different impeller tip clearance, vane count and impeller-diffuser gap. Therefore, the observations would appear to support the hypothesis put forward in section 4.2.

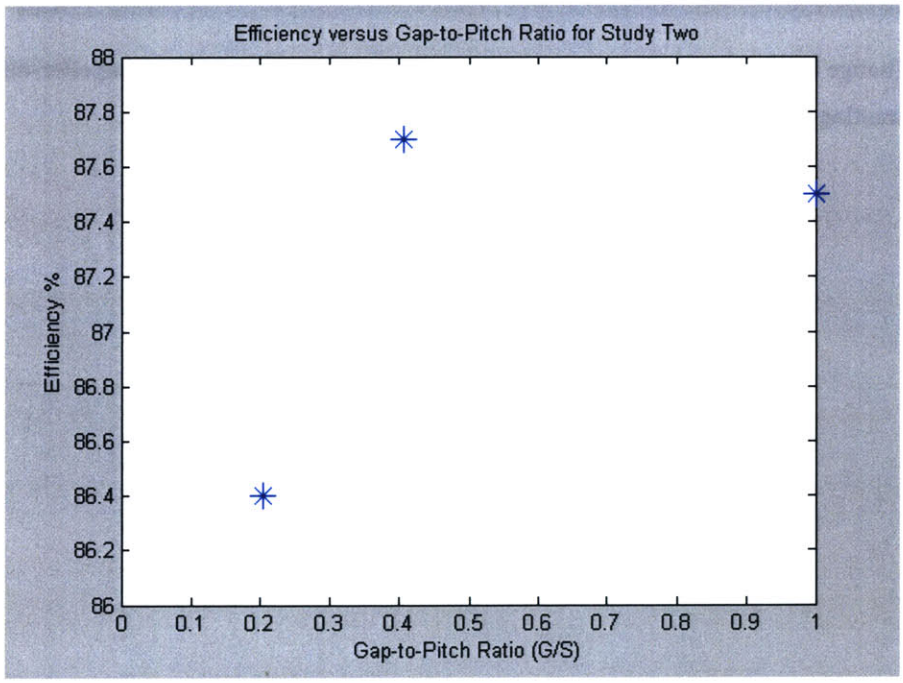

Figure 4-3 Change in impeller efficiency with gap-to-pitch ratio varied through diffuser vane count; the computed trend is non-monotonic.

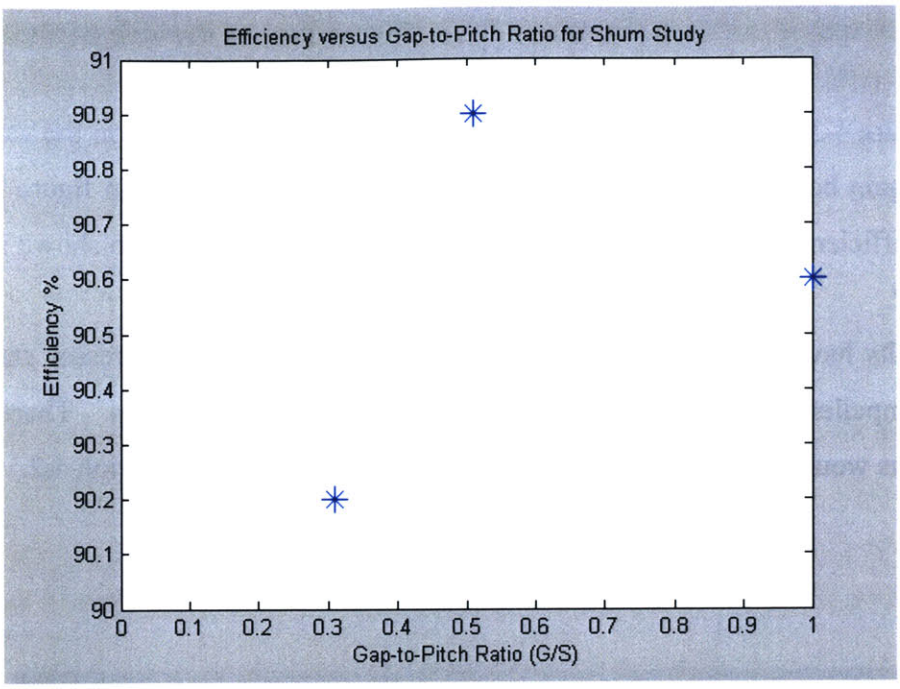

Figure 4-4 Change in impeller efficiency with gap-to-pitch ratio varied through impeller-diffuser gap [21] for contrasting with the results in figure 4-3.

4.4 Summary

The results reported in this chapter appear to show that decreasing the vane count of a diffuser could have the same effect as decreasing the gap size between the impeller and diffuser. This observation supports the hypothesis that altering the diffuser blade count is analogous to changing the gap size. This hypothesis suggests that the ratio of impeller-diffuser gap to diffuser vane pitch essentially characterizes the effect of the impeller-diffuser interaction on impeller performance. The computed results indicate that the change in impeller performance is non-monotonic with the change in the gap-to-pitch ratio, thus there exists a value of this ratio for which the impeller performance is optimal in terms of efficiency and total pressure ratio.

Chapter 5

Summary and Conclusions

5.1 Summary

Two aspects of impeller-diffuser interactions have been examined in this thesis. The first is the effect of impeller tip clearance variation and the second is the effect of diffuser vane count variation on the time-averaged performance of a centrifugal compressor stage. Dawes [6] *UNNEWT* computational fluid dynamics code for solving Reynolds-averaged Navier-Stokes equations has been used.

To examine the first aspect, the effect of tip clearance variation on the change in performance, between centrifugal compressor stages with vaned and vaneless diffusers is determined. In this, three impeller tip clearances, 0%, 4% and 6% (measured in terms of local blade span) were used and results showed that the change in performance had a non-monotonous dependency on impeller tip clearance. The results indicated the existence of a tip clearance where the change in impeller performance between centrifugal compressor stages with vaned and vaneless diffusers is a maximum. The impact of unsteady impeller-diffuser interaction, primarily through the impeller tip clearance flow, is reflected through a time-averaged change in impeller loss, blockage and slip. It is the variation in loss and blockage with tip clearance in the presence of a downstream diffuser that is responsible for the observed trend. The vaned diffuser performance was shown to be dominated by the inlet flow alignment to the diffuser vanes, in accord with previous work [18,21].

A procedure is proposed and developed for isolating impeller passage blockage change without the need to define the region of blockage generation. This method has been assessed for its applicability and utility.

During the course of the flow field analysis in the first study, an interesting phenomenon was identified that could constitute a major source of loss in the CC3 compressor operating at design. Tip flow back leakage was observed and was shown to be a major source of entropy production in the impeller passage. This flow phenomenon is described as tip flow that originates in one passage, flows downstream of the impeller trailing edge and then returns upstream of the impeller trailing edge of a neighboring passage.

In examining the second aspect, three different vane counts were used, 0, 15 & 30, in conjunction with a 6% tip clearance impeller. A hypothesis was put forward that the effect of diffuser vane count on the impeller performance was analogous to the effect of the radial impeller-diffuser gap on the impeller performance. Based on this hypothesis the ratio of impeller-diffuser gap to diffuser vane pitch would essentially set the influence of diffuser vane count as well as the variation in impeller-diffuser gap on impeller performance. Computed results and those by Shum [21] supported the hypothesis and indicated that there exists a blade count or an impeller-diffuser gap and hence a gap-to-pitch ratio that optimizes the performance of the impeller.

5.2 Conclusions

The conclusions are as follows:

1) The change in performance of a centrifugal impeller due to a downstream vaned diffuser is dependent upon the tip clearance.

The results from this study show that an impeller with a downstream vaned diffuser will have a different performance than that of an identical impeller but with a vaneless diffuser. The difference in performance was shown to be dependent on the impeller tip clearance.

2) Tip clearance back-flow can occur at design speeds.

The computed flow fields showed that tip clearance back-flow, originally identified by Vo [26] as occurring at near stall, could occur at design speeds. Back-flow was shown to occur and was seen as a source of high entropy generation (i.e. a source of loss) in the impeller passage.

3) Changing radial gap distance between impeller and diffuser is analogous to changing the diffuser blade count. Thus one may deduce that the gap-to-pitch ratio would essentially characterize the effect of the impeller-diffuser interaction on performance.

4) The vaned diffuser is sensitive to impeller tip clearance change.

The results from this study show that the performance of the diffuser is dependent on the tip clearance of the impeller. The major reason for this is that the mean flow direction at

impeller trailing edge is dependent on the tip clearance. The diffuser performance is in turn dependent on the mean flow angle.

The implications of results on centrifugal compressor designs are as follows:

1) If the performance in the impeller of an impeller-vaned diffuser stage is to be optimized the running tip clearance must be accurately predicted. The dependency of the impeller performance on tip clearance as shown in this thesis dictates that the running tip clearance must be known before the impeller-diffuser interaction can be optimized.

2) Results from this thesis show that the effect on the impeller-diffuser interaction of the diffuser vane count and impeller-diffuser gap size is similar and can then be characterized by the gap-to-pitch ratio. If this is the case, the vane count and gap size can be changed in a such a manner so as to optimize the stage performance. As such this provides some degree of flexibility in sizing the impeller-diffuser gap and in selecting the vane count during the course of designing a centrifugal stage.

5.3 Recommendations for Future Work

The following research tasks are recommended for future research:

(i) The author is of the opinion that a research effort on proving the hypothesis that the gap-to-pitch ratio can characterize the effect of the impeller-diffuser interaction on an unequivocal basis should be undertaken. This research would consist of changing the radial gap size between the impeller and diffuser for the 30 and 15 vane count geometries so that a range of different performances can be assessed in terms of the gap-to-pitch ratio.

The author also recommends that an investigation of different designs be undertaken as well. The objective is to prove the hypothesis that the gap-to-pitch ratio can characterize the effect of the impeller-diffuser interaction on an unequivocal basis.

(ii) It is of engineering interest that a study be undertaken to understand the source of tip leakage back flow. This flow phenomenon is a source of additional entropy production in the impeller and is therefore an un-desirable flow feature. An understanding of how this feature occurs will be of value in designing compressors to avoid this feature.

(iii) Shum [21] and Philips [18] results showed that the performance of the vaned diffuser is predominantly dependent on the alignment of the diffuser vanes with the flow. While the results from this thesis follow this, it is author's opinion that the performance of the vaned diffuser cannot be fully optimized until a thorough research effort into the effect of the impeller-diffuser interaction on diffuser performance is undertaken. The necessity of this research is highlighted in figure 3-29 where the performance of the vaneless diffuser has a non-monotonical dependency on the impeller tip clearance. Thus there is a situation where the performance of the diffuser is optimized

Bibliography

[1] Aknouch, S. Personal Communication, 2002.

[2] Anderson, J.D. *Fundamentals of Aerodynamics 3rd Edition.* McGraw-Hill, 2001

[3] Brasz, J.J. "Investigation into the Effect of Tip Clearance on Centrifugal Compressor Performance." ASME 88-GT-190, 1988.

[4] Came, P.M. & Herbert, M.V. "Design and Experimental Performance of Some High Pressure Ratio Centrifugal Compressors." Paper 15 AGARD Conference *Centrifugal Compressors, Flow Phenomena and Performance*, Brussels, 1980.

[5] Cumpsty, N.A. *Compressor Aerodynamics.* Longman Scientific & Technical, 1989.

[6] Dawes, W. *The Solution Adaptive 3D Navier-Stokes Solver "un_NEWT4.1.f".* CFD Solver Code, 1994.

[7] Dean, R.C., Senoo, Y. "Rotating wakes in Vaneless Diffusers." ASME Journal of Basic Engineering Vol. 82, 1960.

[8] Deniz, S. "Effects of Inlet Conditions on Centrifugal Diffuser Performance." PhD Thesis, Massachusetts Institute of Technology, 1997.

[9] Douglas, J.F., Gasiorek, J.M. & Swaffield, J.A. *Fluid Mechanics 3rd Edition.* Longman Group Limited, 1995.

[10] Filipenco, V., Deniz, S., Johnston, J.M., Greitzer, E.M., Cumpsty, N.A. "Effects of Inlet Flow Field Conditions on the Performance of Centrifugal Compressor Diffusers, Part 1: Discrete-Passage Diffuse." Transactions of the ASME, Vol. 122, No. 1, 2000.

[11] Graf, M.B. "Effects of Stator Pressure Field on Upstream Rotor Performance." PhD Thesis, Massachusetts Institute of Technology, 1996.

[12] Greitzer, E.M., Spakovszky, Z.S., Tan, C.S. Internal Flows in Turbomachinery Class Notes, Massachusetts Institute of Technology.

[13] Japikse, D. "The Influence of Diffuser Inlet Pressure Fields on the Range and Durability of Centrifugal Compressor Stages." AGARD Conference *Centrifugal Compressors, Flow Phenomena and Performance*, Brussels, 1980.

[14] Japikse, D. *Centrifugal compressor Design and Performance.* Concepts ETI Inc., 1996.

[15] Johnston, J.P. *Radial-Flow Turbomachinery.* Lecture Notes Stanford University, 1983.

[16] Kerrebrock, J.,L. *Aircraft Engines and Gas Turbines Second Edition.* The MIT Press, 1992.

[17] Khalid, S.A.. "The Effects of Tip Clearance on Axial Compressor Pressure Rise." PhD Thesis, Massachusetts Institute of Technology, 1995.

[18] Philips, M. "Role of Flow Alignment and Inlet Blockage on Vaned Diffuser Performance." Masters Thesis, Massachusetts Institute of Technology, 1997.

[19] Senoo, Y. "Pressure Loss due to the Tip Clearance of Impeller Blades in Centrifugal and Axial Blowers." Journal of Engineering for Gas Turbines and Power (Vol. 108, No. 1, 1986.

[20] Senoo, Y. "Pressure Losses and Flow Field Distortion Induced by Tip Clearance of Centrifugal and Axial Compressors." JSME Vol. 30, No 261, 1987.

[21] Shum, Y.K. "Impeller-Diffuser Interaction in Centrifugal Compressors." PhD Thesis, Massachusetts Institute of Technology, 200."

[22] Shum, Y.K., Personal Communication, 2002.

[23] Skoch, G., Prahst, P.S., Wernet. M.P., Wood, J.R., Strazisar, A.J. "Laser Anemometer Measurements of the Flow Field in a 4:1 Pressure Ratio Centrifugal Impeller." Army Research Laboratory Technical Report ARL-TR-1448, 1997.

[24] Skoch, G. Personal Communication, 2002.

[25] Tan, C.S. Personal communication, 2002.

[26] Vo, H.D. "Role of Tip clearance on Axial Compressor Stability." PhD Thesis, Massachusetts Institute of Technology, 2001.

[27] Fieldview Revision 8.0. Intelligent Light, 2001.